DISSERTATIONES
CHIMICAE
UNIVERSITATIS
TARTUENSIS
239

MARTA-LISETTE PIKMA

Exploring the basicity of phosphanes and related compounds

DISSERTATIONES CHIMICAE UNIVERSITAS TARTUENSIS
239

DISSERTATIONES CHIMICAE UNIVERSITAS TARTUENSIS
239

MARTA-LISETTE PIKMA

Exploring the basicity of phosphanes and related compounds

UNIVERSITY OF TARTU
Press
1632

Institute of Chemistry, Faculty of Science and Technology, University of Tartu, Estonia

Dissertation is accepted for the commencement of the degree of Doctor of Philosophy in Chemistry on June 10th, 2025, by the Council of Institute of Chemistry, Faculty of Science and Technology, University of Tartu

Supervisors: Associate Prof. Agnes Kütt (PhD)
Institute of Chemistry, University of Tartu, Estonia

Prof. Ivo Leito (PhD)
Institute of Chemistry, University of Tartu, Estonia

Opponent: Martin B. Smith (PhD), Senior Lecturer, Chemistry Programme Director
Department of Chemistry, Loughborough University, UK

Commencement: August 27th, 2025 at 10.15, Ravila 14A-1020, Tartu (Chemicum)

Publication of this dissertation is granted by University of Tartu, Estonia.

This work has been partially supported by Graduate School of Functional materials and technologies receiving funding from the European Regional Development Fund in University of Tartu, Estonia.

ISSN 1406-0299 (print)
ISBN 978-9916-27-927-4 (print)
ISSN 2806-2159 (pdf)
ISBN 978-9916-27-928-1 (pdf)

University of Tartu Press
www.tyk.ee

"*Aitäh!*"

– Arkyn Vares

TABLE OF CONTENTS

LIST OF ORIGINAL PUBLICATIONS

I. **Pikma, M.-L.**; Tshepelevitsh, S.; Selberg, S.; Kaljurand, I.; Leito, I.; Kütt, A. pK_{aH} Values and θ_H Angles of Phosphanes to Predict Their Electronic and Steric Parameters. *Dalton Trans*. **2024**, *53* (34), 14226–14236.

II. **Pikma, M.-L.**; Trummal, A.; Leito, I.; Kütt, A. The Impact of Perfluoroalkyl Groups on Phosphane Basicity. *Molecules* **2025**, *30* (10), 2220.

III. **Pikma, M.-L.**; Lõkov, M.; Tshepelevitsh, S.; Saame, J.; Haljasorg, T.; Toom, L.; Selberg, S.; Leito, I.; Kütt, A. Tris(Benzophenoneimino)-Phosphane and Related Compounds. *Eur. J. Org. Chem*. **2023**, *26* (28), e202300453.

Author's contribution

Paper I: Lead author in preparing the manuscript. Performed most of the calculations and some of the measurement experiments.

Paper II: Lead author in preparing the manuscript. Performed all the calculations.

Paper III: Lead author in preparing the manuscript. Performed all the synthesis experiments and some of the measurements and calculations.

ABBREVIATIONS

Ad	Adamantyl
B	Generic abbreviation for the neutral form of a base
BH^+	Generic abbreviation for the protonated form of a base
Bn	Benzyl group
bpi	Benzophenoneimino group
COSMO-RS	Conductor-like Screening Model for Realistic Solvation
CPCM	Conductor-like PCM
Cy	Cyclohexyl group
DFT	Density functional theory
dma	Dimethylamino group
FLP	Frustrated Lewis pair
G	Gibbs free energy
GB	Gas-phase basicity
I−	Substituents with negative field inductive effect
I+	Substituents with positive field inductive effect
IEF-PCM	Integral Equation Formalism PCM
IPCM	Isodensity PCM
K_a	Dissociation constant
KHMDS	Potassium hexamethyldisilazide
L	Ligand
MeCN	Acetonitrile
Mes	Mesityl
Napht	Naphthyl
NMR	Nuclear magnetic resonance
Np	Neopentyl
PCM	Polarizable Continuum Model
pK_a	Negative logarithm of the dissociation constant K_a
pK_{aH}	Basicity value of a base; equal to the pK_a of its conjugate acid
PR_3	Tertiary phosphane
pyrr	Pyrrolidino group
R	Substituent group
Rf	Perfluoroalkyl group
S	Solvent
SH^+	Solvated proton
SM8	Solvation Model 8
SMD	Solvation Model based on Density
SVPE	Surface and Volume Polarization for Electrostatics
TEP	Tolman's electronic parameter
Tf_2NH	Bis(trifluoromethanesulfonyl)amine
THF	Tetrahydrofuran
tmg	Tetramethylguanidino group
UV-Vis	Ultraviolet-visible

INTRODUCTION

In many cases, reactions that appear highly effective on paper can encounter various limiting factors under real-world experimental conditions. Catalysts help overcome such challenges by offering alternative reaction pathways, often accelerating reactions or altering product distributions. Among the most commonly used compounds in homogenous catalysis are transition metal catalysts, which are effective due to their ability to easily donate and accept electrons. These metals are frequently paired with ligands that enhance the catalyst's activity, selectivity, or stability.[1]

One widely used class of ligands is phosphanes, valued for their tuneable electronic and steric properties, which can be tailored through substituent modification to meet specific catalytic requirements. Phosphanes are also relatively easy to synthesize and many of them are commercially available.

The electronic and steric properties of phosphanes are typically characterized using parameters derived from metal-ligand complexes.[2,3] However, such parameters inherently depend on the metal and are more resource-intensive to obtain, whether through synthesis or computational methods. Deriving comparable descriptors from free phosphanes (or their protonated forms) offers a more efficient alternative, particularly useful when screening a large number of potential ligands for catalytic applications. This approach allows for rapid identification of promising candidates for more detailed investigation.

Basicity is a fundamental molecular property, essential for understanding numerous chemical and biochemical processes, and it serves as an indicator of a ligand's electron-donating ability.[4] Phosphanes represent a versatile class of organic bases, with experimentally determined basicities spanning more than 30 orders of magnitude in acetonitrile.[5–8] In addition, other organophosphorus compounds such as phosphazenes and phosphonium ylides are known for their superbasicity and are frequently used as reagents.[6,7,9]

Practical challenges, including solubility issues and unfavourable steric effects, often limit the efficiency of chemical reactions. As a result, the development of new catalysts and reagents is crucial for broadening the range of viable transformations and opening up pathways to previously inaccessible reactions. Given the central role of phosphanes and other organophosphorus compounds as reagents and catalyst components, continued investigation into their properties and the synthesis of novel derivatives is essential for advancing the field.

The aims of this thesis are:

- Gather basicity data of phosphanes into a **comprehensive overview**
- **Fill in the gaps** in the existing basicity data of phosphanes
- Explore replacing traditional electronic and steric descriptors of phosphanes with **simpler alternatives**
- Develop **novel bases**

1. LITERATURE OVERVIEW

1.1. Phosphanes

Tertiary phosphanes (PR_3) are among the few ligands whose electronic and steric properties can be systematically and predictably altered by varying the substituent groups (R).[10] All PR_3 compounds serve as both σ-donors and π-acceptors when acting as ligands. σ-bonding involves the donation of the lone electron pair on the phosphorus atom to an empty metal orbital of σ-symmetry, while π-backbonding refers to the back-donation of electron density from the filled orbitals of the metal into the phosphane's orbitals of the corresponding symmetry.[11] Typically, σ-donation is the prevalent interaction, especially when the phosphane substituents exert a positive field inductive effect (I+). However, substituents with a negative field inductive effect (I−) enhance the extent of π-backbonding within the metal complex, leading to notable changes in the electronic properties of the phosphane ligand.[12]

Prior to the 1970s, almost all behavioural differences of free ligands and their transition-metal complexes were explained solely by electronic effects, neglecting steric factors. Later, awareness of the combined effects grew, and two parameters were introduced to quantify electronic and steric properties of phosphanes – Tolman's electronic parameter (TEP) and the Tolman cone angle.[3]

The electronic effects of PR_3 ligands (L) are characterized by TEP values, based on the carbonyl stretching frequency ν(CO) in $Ni(CO)_3L$ complexes. Tolman compared ν(CO) frequencies using infrared spectroscopy across multiple phosphane-containing $Ni(CO)_3L$ complexes: stronger electron-donating phosphanes increase electron density at the nickel atom, partially transferring this density to the CO group, thus reducing the ν(CO) frequency.[3]

To characterize steric effects, Tolman introduced the ligand cone angle, defined at the apex of a cone centred at the metal atom. The cone surface encompasses the ligand, passing the outermost atoms at their effective van der Waals radii. The cone angle thus describes the steric demand of a ligand.[13] Properties of sterically hindered phosphanes differ from those with smaller cone angles. Bulkier phosphanes result in lower coordination numbers, formation of coordinatively unsaturated metal centres, and sometimes promote metalation.[14]

Phosphanes exhibit basic properties due to the lone electron pair on phosphorus. Primary and secondary alkylphosphanes have basicities (pK_{aH} values) in water ranging from 0 to 5, whereas for simple trialkylphosphanes, these values are between 8 and 9. Generally, a larger number of substituents corresponds to a higher pK_{aH} value, reflecting enhanced basicity.[15] The basicity of phosphanes is crucial as there is a strong positive correlation between their basicity and coordination ability.

1.1.1. Applications

Phosphanes are important organophosphorus compounds with a wide range of applications.[16,17] Various complexes of phosphanes and metal compounds are utilized as catalysts in numerous reactions. Complexes involving gold, ruthenium, nickel, palladium, and copper have been effectively employed to catalyze three-component coupling reactions, alkene metathesis, alkene hydrogenation, polymerization, among others.[18–21] The mechanism usually involves coordination of the metal atom to the reaction centre (e.g., a double bond) and subsequent electron relocation.[1] Phosphanes themselves typically do not participate directly in the catalytic cycle, instead they dissociate from the metal centre at the beginning of the reaction and later re-coordinate to the metal once again.[14,22]

As mentioned before, the main advantage of phosphanes lies in the possibility to fine-tune their electronic and steric properties through substituent modification, allowing adaptation to the specific needs of a given catalytic transformation. Ligand properties can be precisely tailored to enhance both the reactivity and selectivity of metal catalysts. Even minor modifications to the ligand structure can lead to significant changes in catalytic selectivity.[1] Compared to amines, tertiary phosphanes exhibit stronger coordinating ability resulting from reduced steric hindrance around the phosphorus atom due to its larger size.

A significant advancement in phosphane chemistry occurred in 2006 with the discovery of frustrated Lewis pairs (FLPs) by Douglas W. Stephan's research group.[23] FLPs consist of sterically hindered Lewis acid-base pairs that cannot form classical Lewis adducts, resulting in exceptional reactivity. These pairs can activate small molecules, such as hydrogen, undergoing dynamic transitions between neutral and ionic (or zwitterionic) states during reactions. In FLP chemistry, bulky phosphanes can act as Lewis bases, transitioning to phosphonium cations upon activation. Typically, a substituted borane acts as the Lewis acid. The discovery of FLPs has significantly impacted modern chemistry, notably accelerating the development of metal-free hydrogenation catalysis.[24] A critical factor to consider about FLPs is the basicity of the phosphane – phosphanes with high basicity bind protons too strongly and do not release them efficiently, while weakly basic phosphanes lack the capability to activate hydrogen effectively.[8] This highlights the importance of determining the basicity of phosphanes and also designing novel phosphanes with precisely tailored basicities.

1.1.2. Preparation

Due to the significant role of phosphanes in catalysis, multiple synthetic methods have been developed for functionalized phosphanes.[25] The three prevalent methods are: 1) reactions between organometallic compounds and halogenophosphanes, 2) reactions of metal phosphides with alkyl halides, and 3) the reduction of other phosphorus-containing compounds.[26]

The main synthetic pathway for symmetrical tertiary phosphanes involves halogen substitution in halogenophosphanes (typically PCl_3 or PBr_3) using organometallic reagents due to the readily available precursors. This method was used in this work as well. Frequently used organometallic reagents include Grignard and lithium reagents. However, the applicability of this method is restricted by the nucleophilic carbon, meaning the desired phosphane cannot contain functional groups reactive with the chosen organometallic reagent.[27] Another limitation arises from phosphanes' propensity to form stable complexes with some salts (byproducts here). In this case, the phosphane itself is no longer the product but rather the phosphane complex. In some instances, heating the reaction mixture in solvents in which the salt is insoluble can help recover the free phosphane. When applicable, complex formation may be avoided by selecting alternative solvents or reagents.[7]

1.2. Phosphazenes and phosphonium ylides

Phosphazenes are derivatives of phosphanes with the general structure $RN{=}PR_3$. These compounds exhibit a degree of zwitterionic character, meaning the N=P double bond can be interpreted either as a formal double bond (ylenic form) or as a single bond between oppositely charged atoms (ylidic form).[28] This is also the case for phosphonium ylides, which have a similar structure to phosphazenes, but with a carbon atom in place of the nitrogen. These are typically represented as $RHC^{-}{-}P^{+}R_3$, as the ylidic form is generally the dominant one.[29,30]

Phosphazenes and phosphonium ylides are well-known for their strong basicity, with many classified as superbases.[31–33] Phosphonium ylides are usually around 10 pK_{aH} units stronger bases than the analogous phosphazenes.[9] This is due to the unstable nature of the carbanion (R_3C^-) compared to R_2N^-, making phosphonium ylides comparatively more prone to protonation.

1.3. Basicity of compounds

The ability of a compound to donate or accept a proton represents one of its most fundamental chemical properties. This characteristic is referred to as Brønsted-Lowry acidity or basicity, respectively, and its accurate quantification is crucial for understanding numerous chemical and biochemical processes.[34] Namely, it provides insight into the ability of the compound to activate other species within a reaction mixture and determines the predominant form of the compound under given conditions.

1.3.1. Gas- and solvent-phase basicities

Gas-phase basicity (GB) is defined as the change in Gibbs free energy (G) of the following reaction:

$$BH^+ \overset{GB}{\rightleftarrows} B + H^+ \quad (1)$$

where B denotes the base under investigation and BH^+ is its conjugate acid. GB value is obtained as follows:

$$GB = G(B) + G(H^+) - G(BH^+) \quad (2)$$

where $G(H^+) = -6.275$ kcal·mol^{-1}.[35]

GB values are usually expressed in kcal·mol^{-1} and higher GB values mean stronger basicities. Despite its fundamental significance, gas-phase basicity does not accurately reflect the situation in solution, since solvent effects are of importance depending on the solvent and the type of base.[36] In particular, the conjugate acid of a base can experience additional stabilization in solution, which is absent in the gas phase. The acid-base equilibrium describing the basicity of a base B in a solvent S is as follows:

$$BH^+ + S \overset{K_a}{\rightleftarrows} B + SH^+ \quad (3)$$

where BH^+ is the conjugate acid of the base B and SH^+ is the solvated proton.

The basicity of a compound in a solvent is quantified by the pK_a value of its conjugate acid, which is the negative logarithm of its dissociation constant (K_a):

$$pK_a = -\log K_a = -\log \frac{a(SH^+) \cdot a(B)}{a(BH^+)} \quad (4)$$

where $a(SH^+)$, $a(B)$ and $a(BH^+)$ are the activities of the corresponding species.

Higher pK_a value indicates greater basicity. It has been proposed[37] to denote the basicity of base B as its pK_{aH} instead of expressing its basicity as the pK_a of its conjugate acid BH^+: $pK_{aH}(B) \equiv pK_a(BH^+)$. In this work, all basicities in solvent are denoted as pK_{aH}.

1.3.2. Measuring pK_{aH} values

Since measuring the activity of the solvated proton $a(SH^+)$ is difficult in non-aqueous media,[38] the relative basicity measurement method is often employed instead of absolute measurements, such as those based on potentiometry. In relative measurement, the basicity of the base under investigation is compared in the same solution with the basicity of another base with a known pK_{aH} value,

and the difference in their pK_{aH} values (ΔpK_{aH}) is determined experimentally. As a result, the effects arising from water, ionic strength, and other interfering factors are either partially or fully cancelled out, providing an additional advantage of employing the relative measurement method.[39]

Using this approach, a self-consistent scale of relative basicities is established, anchored to a compound possessing an absolute pK_{aH} value determined with the highest possible precision. Typically, this implies that the absolute pK_{aH} value of the anchor compound has been determined using multiple independent methods, yielding consistent and closely agreeing results. For example, the current pK_{aH} scale in MeCN is anchored to pyridine (pK_{aH} = 12.53).[4] The relative measurement method is based on the following equilibrium:

$$B_1 + B_2H^+ \overset{K}{\rightleftarrows} B_1H^+ + B_2 \qquad (5)$$

where B_1 and B_2 are the two bases in the same solution and B_1H^+ and B_2H^+ are their conjugate acids. The relative basicity (ΔpK_{aH}) of the bases B_1 and B_2 is defined as follows:

$$\Delta pK_{aH} = pK_{aH}(B_1) - pK_{aH}(B_2) = \log K = \log \frac{a(B_1H^+) \cdot a(B_2)}{a(B_2H^+) \cdot a(B_1)} \qquad (6)$$

where $a(B_1H^+)$, $a(B_2H^+)$, $a(B_1)$, and $a(B_2)$ are the activities of the corresponding species. Given that it is justified to assume here that the ratios of activity coefficients are the same for both studied bases,[40] the ratios of activities can be replaced by ratios of equilibrium concentrations.

In general, pK_{aH} can be determined using any method that allows the quantitative measurement of a parameter sensitive to the pH of the surrounding environment. Among others, UV-Vis spectrometry is one of the most widely used methods for determining relative pK_{aH} values.[5,6,39–42] Its appeal lies in its simplicity and robustness, as well as its capability to operate effectively at very low concentrations. However, UV-Vis spectrometry has limitations, including the requirements for UV-Vis active groups and for the purity of the compounds (especially, the absence of UV-absorbing acidic/basic impurities).

The challenges presented by UV-Vis spectrometry may be circumvented by using nuclear magnetic resonance (NMR) spectroscopy,[5,43,44] which can be applied to a wider variety of compounds. When using ^{1}H NMR, the only structural requirement is the presence of a hydrogen atom. Additionally, impurities do not pose a significant issue, as ^{1}H NMR provides well-resolved peaks corresponding to specific protons in the molecular structure, rather than a collective representation of the entire molecule, as is the case in UV-Vis spectroscopy.

Another advantage of using NMR is the ability to simultaneously measure more than two bases within a single experiment. This enables the determination of two distinct ΔpK_{aH} values (against two different reference bases) for the base

of interest, as well as an additional ΔpK_{aH} value between the two reference bases. The latter serves as an internal control, providing a means to assess the reliability and consistency of the measurement. A drawback of NMR spectroscopy is its requirement for higher sample concentrations compared to the UV-Vis method.

1.4. Computational methods

Experimental investigations can be highly resource-intensive, both in terms of cost and time. Moreover, certain systems or conditions remain inaccessible to experimental techniques, at least with current technological capabilities. Even fundamental factors such as solubility can hinder empirical studies.

In such cases, computational methods offer practical alternatives and have seen widespread adoption.[5,45–48] While computational approaches may not match the accuracy of experimental methods – particularly in solution-phase studies – they still provide valuable insights. In many instances, achieving the highest absolute accuracy is not essential, especially when relative values are sufficiently informative. Computational methods are particularly valuable when used in conjunction with empirical data, as the combination can yield reasonably accurate and reliable results.

1.4.1. Density functional theory

Density functional theory (DFT) is a quantum mechanical method used to investigate the electronic structure of molecules and other systems. DFT is one of the most widely employed methods in computational chemistry due to its balance between accuracy and computational efficiency. It offers higher accuracy than the Hartree-Fock (HF) method, which neglects electron correlation (the mutual influence of electrons on each other) while being less resource-demanding than post-HF methods that rely on many-body electronic wavefunctions.[51,52]

DFT is based on the principle that all ground-state properties of an electronic system are determined by its ground-state electron density, and that the energy of this electron distribution can be expressed as a functional of the electron density. The optimal electron density corresponds to energy minimum, i.e. to the ground-state energy of the system.[49,50]

While orbital-free DFT is appealing in theory, it remains limited in practice owing to the lack of reliable approximations for the kinetic energy functional. Consequently, Kohn-Sham DFT is more commonly employed. In this approach, the electronic kinetic energy is estimated by populating non-interacting single-particle orbitals with electrons. Since the kinetic energy of non-interacting electrons can be calculated exactly, the Kohn-Sham framework enables more accurate DFT computations by reducing the portion of the kinetic energy that must be approximated. Although the fictious non-interacting reference system shares the same electron density as the true interacting system, its kinetic energy does not fully capture that of the real system due to the absence of electron-

electron interactions. The residual part of the true kinetic energy is incorporated into the exchange-correlation energy of the system in addition to the effects of self-interaction correction (accounts for the fact that an electron does not interact with itself), exchange (reflects the Pauli exclusion principle, which prevents two electrons with the same spin from occupying the same region of space), and correlation (describes the dynamic interactions between electrons due to their mutual repulsion).[51]

A key challenge in DFT is the formulation of the exchange-correlation functional.[51] Since the exact form of this functional is known only for idealized systems, such as the free electron gas,[49] numerous approximations have been developed. The choice of functional depends on the system under investigation and the specific properties of interest. For example, some functionals are better suited for small molecules, while others perform better for extended systems or interfaces.

In addition to functionals, the selection of a basis set is important in DFT calculations. A basis set is a collection of mathematical functions used to describe the spatial distribution of electrons in a system. These sets allow the transformation of the model's partial differential equations into algebraic equations, making them solvable on a computer. The choice of basis set, like the functional, influences the accuracy and computational cost of the calculation.[53] In theory, achieving the highest accuracy would involve employing the largest and most comprehensive basis set available for modelling molecular orbitals. However, in practice, the computational cost increases rapidly with the size of the basis set, often making such calculations impractical for larger or more complex systems. As a result, considerable effort has been devoted to evaluating and benchmarking different basis sets to identify those that offer the best compromise between accuracy and computational efficiency.[54,55] The optimal choice of basis set is context-dependent, contingent upon both the property being calculated and the specific molecular system under investigation.

1.4.2. Dielectric continuum solvation models

In vacuo, molecular properties are determined solely by the intrinsic structural and electronic characteristics of the molecular system. Conversely, calculations in fluid environments must also account for intermolecular interactions with the surrounding medium. Explicitly modelling solvent molecules around the solute can be extremely resource-intensive, since computational cost increases significantly with system size.

To address this challenge, dielectric continuum models have gained popularity. In these approaches, the solvent is treated as a homogeneous medium characterized by relative permittivity (i.e., dielectric constant), greatly simplifying the system while still capturing essential solvent effects. The cavity for the solute is generated based on its intrinsic Coulomb radii, which define the spatial extent of the solute.[56]

Different dielectric continuum models include Polarizable Continuum Model (PCM),[56] Conductor-like PCM (CPCM),[57,58] Isodensity PCM (IPCM),[59] Integral Equation Formalism PCM (IEF-PCM),[60–63] Solvation Model based on Density (SMD),[64] Solvation Model 8 (SM8),[65] Surface and Volume Polarization for Electrostatics (SVPE),[66–68] etc. For the calculation of solvation free energies (which are essential for determining pK_{aH} values in the solvent phase), the SMD model is currently the recommended approach when using the Gaussian software package. The SMD model is based on the quantum mechanical charge density of the solute molecule (hence the "D" in SMD) and on a continuum model of the solvent.[64]

In cases where strong hydrogen bonds form between solute and solvent molecules, implicit solvation models (like the ones mentioned above that account only for bulk polarization effects) are often insufficient, as they neglect first-layer solvation effects arising from short-range solute-solvent interactions. These specific interactions can be addressed by explicitly including one or several solvent molecules in the solute structure prior to applying a dielectric continuum model – this is called the "cluster-continuum" approach.[69] In addition to aqueous solutions, which typically display strong specific solvation effects, the inclusion of explicit solvent molecules has also been shown to improve accuracy in other polar and especially in protic organic solvents. In contrast, for aprotic solvents such as acetonitrile (MeCN) and tetrahydrofuran (THF), implicit solvation models alone generally yield more reliable and accurate results.[48]

1.4.3. COSMO-RS

The Conductor-like Screening Model for Realistic Solvation (COSMO-RS) is a hybrid method that combines a dielectric continuum solvation model with statistical thermodynamics.[70] In the first step, the molecule is calculated using DFT within an ideal conductor environment ($\varepsilon = \infty$), yielding its geometry, total energy, and charge distribution on the molecular surface. Subsequently, the molecule is conceptually transferred from the ideal conductor to a real solvent environment using statistical thermodynamics.[71]

The molecular surface is partitioned into small segments, each characterized by specific coordinates, surface area, and surface charge density (σ-potential). Electrostatic interactions are captured through pairwise interactions between surface segments. A hydrogen bond is considered to be present between two species when one has a hydrogen atom with highly negative σ-potential, the other one a moiety with highly positive σ-potential, and the difference of these respective charge densities exceeds a defined threshold value. Its contribution is quantified on the basis of the respective polarization charge densities. Dispersion forces are incorporated via a dedicated dispersion term.[71]

A notable strength of COSMO-RS is that it does not distinguish between solute and solvent molecules – all species are treated on an equal footing. Interactions between solute molecules, as well as solvent-solute and solvent-solvent

interactions, are included, allowing for the treatment of concentrated solutions and multi-component solvent mixtures.[72] Unlike many other solvation models, COSMO-RS does not rely on solvent-specific parametrizations. Instead, its parametrization is based on atomic properties, general parameters applicable across a broad range of systems and specific parameters for some computations (e.g., pK_a values).

Despite these advantages, COSMO-RS has limitations. While it is highly effective for predicting relative trends, it is not the most reliable method for absolute results without correlation to experimental data. Furthermore, each new version of the software introduces updated parametrizations and it has been demonstrated that the predictive accuracy of COSMO-RS is highly dependent on the specific parametrization employed.[5]

2. EXPERIMENTAL SECTION

Descriptions of the used instruments and software, as well as the origins of the compounds, are provided in papers I, II, and III. This section offers a brief overview of the experimental procedures; for comprehensive details, the reader is referred to the respective publications.

2.1. Basicity measurements

UV-Vis spectrophotometric titration method

For most of the compounds, the relative pK_{aH} measurement method using UV-Vis spectrophotometric was employed. If the protonation centre is sufficiently close to the part of the molecule responsible for UV-Vis absorbance (the chromophore), then the UV-Vis spectra of the protonated and deprotonated forms of the molecule are expected to differ significantly, enabling reliable pK_{aH} measurements.

Initially, individual titrations are carried out for each base to acquire the spectra of their respective deprotonated and protonated forms. This allows for identification of the spectral shape and observation of how the spectrum of the base changes upon protonation. Additionally, any potential interference from impurities can be detected at this stage. Subsequently, both bases are titrated together in the same solution. During this combined titration, a larger number (typically 15 to 30) of spectra of partially protonated bases are recorded, with smaller increments of titrant added per step. The ΔpK_{aH} value is then determined as an average of values obtained via multilinear regression analysis from the individual spectra of partially protonated bases. Detailed description of the methodology is provided in the supporting information of paper III and ref 42. The author conducted the UV-Vis titration measurement of benzophenoneimine, while the remaining UV-Vis measurements were performed either by Märt Lõkov or Agnes Kütt.

NMR titration method

For some of the relative pK_{aH} measurements, NMR spectrometry was used. Detailed description of the methodology is presented in paper I. The author performed all NMR titration measurements.

When using NMR for pK_{aH} measurements, it is not necessary to measure the NMR spectra of the pure compounds if their structures are sufficiently distinct to allow for clear interpretation of the mixture spectrum. In principle, the identification of a single, well-resolved peak per compound is sufficient for the analysis. However, it is beneficial to record the spectra of the fully deprotonated and protonated forms of the mixture in separate tubes prior to titration (Scheme 1), instead of getting this information at the end of the titration from the first and last titration spectra corresponding to the fully deprotonated and protonated forms. This provides valuable insight into the ratio of protonated to deprotonated

species during the titration, which can be particularly useful for determining the appropriate amount of titrant to add before recording the next spectrum. Such real-time assessment helps optimize the measurement for data quality and ensures that spectra are collected across a suitable range of protonation states. While the volume of titrant added can also offer an indication of this ratio, it is generally less accurate than direct spectral observation.

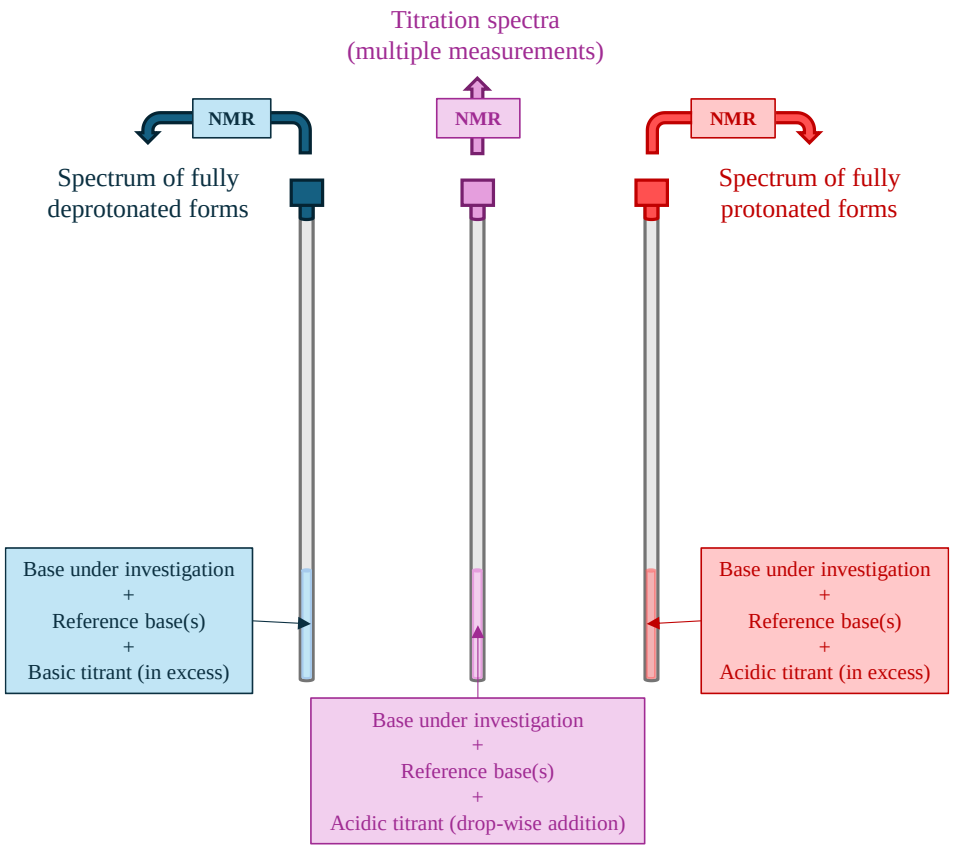

Scheme 1. Relative pK_{aH} measurement with NMR in this work.

For accurate pK_{aH} determination, the protonation centre should be sufficiently close to the NMR-active nucleus (most often, hydrogen) selected for the calculations. In the case of ^{1}H NMR, this requirement is typically not a limitation, as most organic compounds contain numerous hydrogen atoms and usually at least some of them have suitable peaks for analysis. Problems can arise from the solvent peaks, which are significantly more intense than those of the analytes, especially when non-deuterated solvents are used. If the signals of the studied bases are too close to the solvent peak, they may become obscured during titration due to chemical shift changes, complicating data interpretation. In such cases, the use of a deuterated solvent is possible to suppress the solvent signal (in this work, MeCN-d_3 was used as the solvent for the pK_{aH} measurement of

PCy_3). However, when spectral overlap is not a concern, non-deuterated solvents are often preferred due to their lower cost. While the absolute pK_{aH} values may differ slightly between deuterated and non-deuterated solvents, the ΔpK_{aH} value remains virtually unchanged, as both bases are affected similarly by the solvent environment.

Sometimes broadening (or even disappearance) of peaks can occur during titration if the added proton at the basic centre is coupled to the one corresponding to the peak under investigation and proton exchange occurs at an intermediate rate on the NMR timescale.[73] In this regime, the nuclei experience fluctuating chemical environments that are neither fully averaged, as in the case of fast exchange, nor clearly distinct, as in slow exchange. This phenomenon was observed for some phosphanes measured in this work. To ensure reliable analysis, at least three spectra (ideally five or more) were acquired that displayed suitable ratios of protonated to deprotonated forms (between 0.1–0.9) within a single measurement.

2.2. Quantum chemical calculations

This section provides an overview of the computational procedures carried out in this work. Specific details regarding the computational methods and levels of theory employed are provided in papers I, II, and III. The author performed most of the quantum chemical calculations, some of the calculations in papers I and III were carried out by Sofja Tšepelevitš.

General procedure

First, the structures were optimized using the level of theory specified in each respective paper. Providing a reasonable starting geometry for the calculation is crucial, as unrealistic structures can prevent proper convergence. It is particularly important to avoid specifying linear arrangements where angular geometries are expected, as this can hinder reaching the optimal geometry and lead to inaccurate results. For example, if a linear geometry is submitted for a water molecule, the optimization will not successfully yield the correct bent structure.

Following geometry optimization, a frequency calculation was done to verify whether the resulting structure corresponded to a true minimum on the potential energy surface. A true minimum is characterized by the absence of imaginary frequencies, whereas the presence of one or more imaginary frequencies indicates a slope on the potential energy surface, a transition state or a higher-order saddle point. If imaginary frequencies were detected, the geometry was reoptimized following a slight reorganization of the structure, typically involving adjustment of the phosphorus atom in the case of phosphanes. In certain instances, it was also necessary to impose additional constraints or modify specific computational parameters to achieve a true minimum.

If multiple conformers are possible for the molecule under investigation, all relevant conformers should be evaluated to determine the one with the lowest

energy. This can be done manually by generating reasonable conformational guesses or more efficiently using specialized software designed for conformer generation and analysis. Identifying the lowest-energy conformer is essential, as it most accurately represents the thermodynamically preferred structure for further calculations. In this work, conformer searches were performed using COSMOconf[74] (BP86/def-TZVP level of theory) for all calculations. The conformer with the lowest energy was then subjected to geometry optimization at the desired level of theory.

Calculation of pK_{aH} values in solvent phase

A simplified workflow for the calculation of pK_{aH} values employing either the SMD or COSMO-RS model is illustrated in Scheme 2 and explained below:

SMD vs COSMO-RS

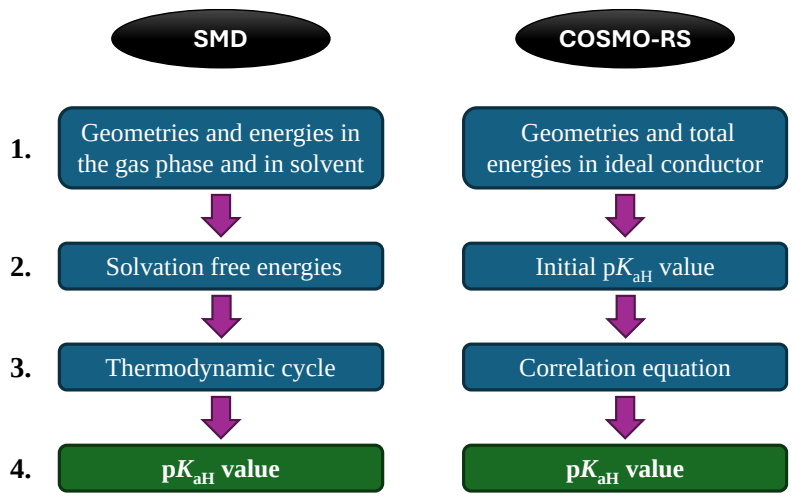

Scheme 2. Simplified workflow of pK_{aH} calculations using SMD and COSMO-RS models in this work.

SMD model

1. Calculation of geometries and SCF energies for neutral and ionic species in the gas phase and in solvent (SMD model was used for the latter).
2. Calculation of solvation free energies as the differences in SCF energies of the structures in the gas phase and in solvent.
3. The thermodynamic cycle (Scheme 3) of proton exchange between two bases (base under investigation B_1 and a reference base B_2) is applied using the solvent free energies obtained from gas- and solvent-phase structures according to the following equations:

$$pK_{aH}(B_1) = pK_{aH}(B_2) + \frac{\Delta G_{soln}}{RT\ln(10)} \quad (7)$$

$$\Delta G_{soln} = \Delta G_{gas} + \Delta G_{solv}(B_1) - \Delta G_{solv}(B_1H^+) - \Delta G_{solv}(B_2) + \Delta G_{solv}(B_2H^+) \quad (8)$$

4. pK_{aH} value is obtained from equations 7 and 8.

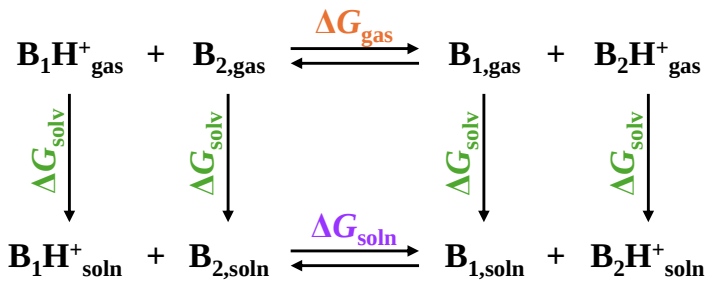

Scheme 3. Thermodynamic cycle of proton exchange between two bases B_1 and B_2; B_1H^+ and B_2H^+ are their conjugate acids. Subscript "gas" indicates the gas phase, "soln" indicates the solvent phase. ΔG_{solv} is the solvation free energy.

COSMO-RS model

1. Calculation of compound's geometry, charge/σ-potential distribution and total energy (stored as COSMO files) for neutral and ionic species in ideal conductor.
2. Initial pK_{aH} value is obtained with statistical thermodynamics using the COSMO-RS method (implemented in the COSMOtherm[75] software).
3. Correlation equation is applied (a collection of calculated and experimental pK_{aH} values for similar compounds is needed).
4. Corrected pK_{aH} value is obtained.

Assessment of steric properties of phosphanes

In paper I, it is proposed using either the C–P–C angle (θ_{CPC}) or the exact cone angle of the protonated phosphanes (θ_H) to assess the steric properties of phosphanes (Scheme 4).

The θ_{CPC} angle represents the average of the three C–P–C bond angles in the protonated solvent-phase structure (single C–P–C angle is depicted in Scheme 4). While θ_{CPC} provides a simple and accessible steric descriptor, it does not offer the most realistic representation of the steric bulk of a phosphane. Therefore, θ_H was also proposed, which is similarly derived from the geometry of the protonated phosphane, and describes more realistically the steric demand of the phosphane as ligand. The surface of the cone touches the van der Waals spheres of the outer atoms and the proton is the apex of the cone.

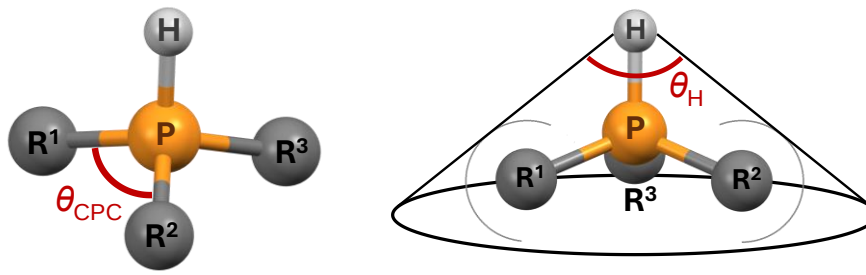

Scheme 4. Single C–P–C bond angle (on the left) and the θ_H angle of a phosphane (on the right). The average θ_{CPC} angle used in this work is calculated using all three single C-P-C angles.

2.3. Synthesis

This section introduces the general synthesis procedures carried out in paper III, where the experiments are described in detail. The author performed all of the synthesis experiments.

Benzophenoneimino (bpi) substituted phosphazenes were prepared by coupling alkyl or aryl azides with the respective tertiary phosphane (Staudinger method[76,77]). Phosphonium salts were synthesized as precursors to phosphonium ylides; however, the resulting ylides proved to be unstable in their free form. Deprotonation of $(bpi)_3P^+–CH_2Ph$ with different bases resulted in the formation of a P–N heterocyclic compound (see below).

General procedure for the synthesis of bpi-substituted phosphazenes (Scheme 5). Tris(benzophenoneimino)phosphane (1 equiv) and an azide (1.2 equiv) were separately dissolved in toluene (approximately 50–100 mg/ml). The solutions were cooled down to 0 ºC. The azide solution in toluene was added dropwise to the phosphane solution, and the reaction mixture was stirred overnight at room temperature. When the reaction was complete, the mixture was

filtered, and the filtrate was added to a 15 ml vial. The vial was carefully filled to the top with hexane and after letting hexane diffuse slowly into the toluene phase at 3 ºC, crystals of phosphazenes were formed. The crystals were filtered off and washed with hexane.

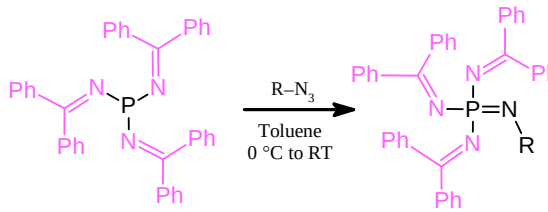

R	
t-Bu–	4-CF_3-C_6H_4–
Ph–	4-Cl-C_6H_4–
4-CH_3O-C_6H_4–	4-$N(CH_3)_2$-C_6H_4–
4-NO_2-C_6H_4–	4-$N(CH_3)_2$-C_6H_4-N=N-C_6H_4–

Scheme 5. Preparation of bpi-phosphazenes.

General procedure for the synthesis of bpi-substituted phosphonium salts (Scheme 6). Tris(benzophenoneimino)phosphane (1 equiv) was dissolved in toluene (30–150 mg/ml) and added to an oven-dried (140 ºC) vial or J Young valve NMR tube in a glovebox. Alkyl or aryl halide (1 equiv) was added, respective halide ion was later the counterion for the resulting phosphonium cation. The reaction mixture was stirred at 60-90 ºC outside of the glovebox under argon. When the reaction was complete, the mixture was filtered to obtain the product as a solid.

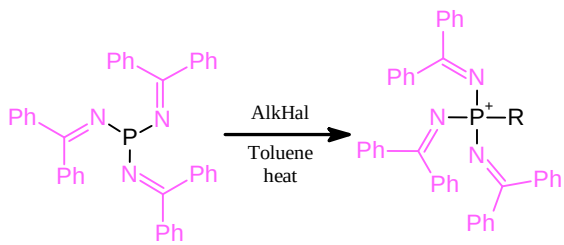

R
–CH_3
–CH_2CH_3
–$CH(CH_3)_2$
–CH_2Ph
–$CH(CH_3)Ph$
–$CHPh_2$

Scheme 6. Preparation of bpi-substituted phosphonium cations.

General procedure for deprotonation of (bpi)$_3$P$^+$–CH$_2$Ph (Scheme 7). *P*-benzyl tris(benzophenoneimino)phosphonium bromide (1 equiv) and toluene (~50 mg/ml) were added to an oven-dried (140 ºC) vial in a glovebox. The solution was cooled down to 0 ºC, and a base (1.1 equiv) was added. The reaction mixture was stirred at 70 ºC outside the glovebox under argon. After 1–3 days, the mixture was filtered in a glovebox. Toluene was removed *in vacuo*, and the

product was extracted with hexane (3 x 4 ml). Hexane was removed *in vacuo*. P–N heterocycle was obtained as a dark violet solid.

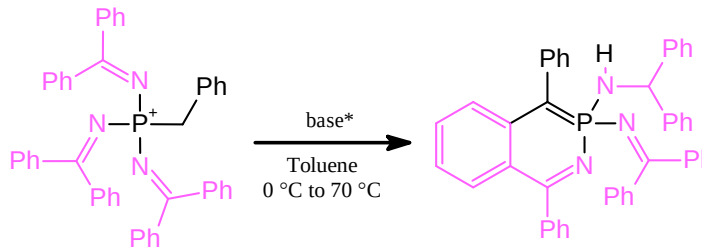

P–N heterocycle

Scheme 7. Deprotonation of (bpi)$_3$P$^+$–CH$_2$Ph. * NaH, KH, KHMDS or *t*-BuOK.

3. RESULTS AND DISCUSSION

3.1. Basicity of organophosphorus compounds

The basicities in the gas phase (GB values) and solvent (pK_{aH} values in acetonitrile) of 80 organophosphorus compounds from papers I, II, and III, along with steric parameters C–P–C (θ_{CPC}) and exact cone angles (θ_H) of phosphanes, are presented in Table 1. The methodologies used to obtain these values are detailed in the Experimental section and the respective papers, as indicated by the superscripts following each compound. All COSMO-RS values in papers I, II, and III were calculated at the same level of theory (BP86/def-TZVP//def2-TZVPD). SMD values in paper II were calculated at SMD/M06-2X/6-31+G(d) level of theory. The GB values from paper II were calculated at a different level of theory (M06-2X/6-31+G(d)//MP2/6-311++G(d,p)) compared to the one in papers I and III (BP86/def2-TZVP//MP2/def2-TZVPP). The θ_{CPC} and θ_H values reported in paper II were mainly calculated using structures optimized with the SMD solvation model, whereas the corresponding values in paper I were derived from structures obtained using the COSMO-RS model.

A total of 15 novel benzophenoneimino substituted compounds were synthesized in this work: experimental pK_{aH} values were measured for 9 of them, while the remaining 6 were evaluated computationally. Additionally, pK_{aH} values were determined for their precursors – $P(bpi)_3$ and benzophenoneimine (bpi-H), computationally for the former and experimentally for the latter. The experimental pK_{aH} values for 12 phosphanes were also reported for the first time. In addition, calculated properties were presented for a total of 63 phosphanes. 13 experimental pK_{aH} values in Table 1 are taken from the literature.

Table 1. Properties of organophosphorus compounds. Compounds are in decreasing order according to COSMO-RS pK_{aH}(MeCN) values.

		pK_{aH}(MeCN)					
No	Compound	experimental	COSMO-RS	SMD	GB [kcal·mol^{-1}]	θ_{CPC} [º]	θ_{H} [º]
1	Me_2C=P(bpi)$_3$ [a]		≤37		284.9		
2	MeCH=P(bpi)$_3$ [a]		≤37		274.7		
3	H_2C=P(bpi)$_3$ [a]		≤36		281.0		
4	Ph(Me)C=P(bpi)$_3$ [a]		≤31		262.7		
5	Ph_2C=P(bpi)$_3$ [a]		≤28		269.9		
6	PhCH=P(bpi)$_3$ [a]		31		267.8		
7	*t*-BuN=P(bpi)$_3$ [a]	25.32			260.8		
8	P[2,4,6-$(MeO)_3$-C_6H_2]$_3$ [b]	19.66	21.4		261.5	114.8	275
9	4-NMe_2-C_6H_4-N=P(bpi)$_3$ [a]	21.31			259.1		
10	4-MeO-C_6H_4-N=P(bpi)$_3$ [a]	20.69			258.5		
11	PhN=P(bpi)$_3$ [a]	20.14			257.0		
12	P(pyrr)$_3$ [b]	20.35	19.5		241.8	111.7	218
13	4-Cl-C_6H_4-N=P(bpi)$_3$ [a]	19.21			257.5		
14	4-NMe_2-C_6H_4-N=N-C_6H_4N=P(bpi)$_3$ [a]	18.99			261.5		
15	PAd$_3$ [b]		18.5		246.2	115.0	244
16	4-CF_3-C_6H_4-N=P(bpi)$_3$ [a]	18.39			252.4		
17	P[2,6-$(MeO)_2$-C_6H_3]$_3$ [b]	17.23	18.2		254.2	114.8	273
18	P(*t*-Bu)$_3$ [b]		17.3		238.1	114.8	244
19	P(dma)$_3$ [b]	18.9	17.1		234.5	111.6	223
20	P-N heterocycle [a] (Scheme 7)	17.06			234.5		
21	4-NO_2-C_6H_4-N=P(bpi)$_3$ [a]	17.00			247.7		
22	PCy$_3$ [b]	16.7	16.6		240.3	112.7	229
23	P[2,4,6-$(MeO)_3$-C_6H_2]$_2$Ph [b]	15.87	16.5		252.6	114.0	252
24	P(bpi)$_3$ [a]		16.0		246.9		
25	P(*i*-Pr)$_3$ [b]		15.7		233.1	112.6	227
26	PMe_2Et [b]		15.6		223.5	111.2	187

[a] from paper III; [b] from paper I; [c] from paper II.

No	Compound	pK_{aH}(MeCN) experimental	COSMO-RS	SMD	GB [kcal·mol^{-1}]	θ_{CPC} [º]	θ_{H} [º]
27	PMe_3 [b]	15.48	15.6	18.5	220.3	110.4	163
28	P(*i*-Pr)$_2$Me [b]		15.3		228.6	111.9	219
29	$PMeEt_2$ [b]		15.1		225.4	111.4	187
30	P(*n*-Pr)$_3$ [b]		15.0		229.5	111.6	215
31	PEt_3 [b]		14.8		226.8	111.5	212
32	P(*n*-Bu)$_3$ [b]		14.7		230.0	111.5	213
33	P(*t*-Bu)$_2$Ph [b]		14.7		236.1	114.3	243
34	bpi-H [a]	13.92			230.6		
35	P(*i*-Bu)$_3$ [b]		13.8		229.7	110.9	250
36	PCy_2Ph [b]		13.1		235.1	112.4	225
37	$PMes_3$ [b]	12.87	13.0		239.5	115.9	302
38	PNp_3 [b]		12.8		231.3	110.0	284
39	PEt_2Ph [b]		12.7		228.2	111.7	218
40	P(*n*-Bu)$_2$Ph [b]		12.6		231.8	111.7	219
41	PMe_2Ph [b]	12.64	12.2		224.4	111.2	198
42	P[2,4,6-(MeO)$_3$-C_6H_2]Ph_2 [b]	11.76	11.5		241.5	113.2	237
43	P(*t*-Bu)Ph_2 [b]		11.4		232.6	113.6	241
44	P(4-MeO-C_6H_4)$_3$ [b]	10.06	10.5		239.5	111.9	216
45	$PEtPh_2$ [b]		10.1		227.3	111.8	224
46	$PCyPh_2$ [b]	10.23	10.0		231.3	112.4	232
47	P(2-MeO-C_6H_4)$_3$ [b]		9.8		241.4	110.7	248
48	$PMePh_2$ [b]	9.97	9.5		226.5	111.4	202
49	PBn_3 [b]		9.3		229.1	112.0	250
50	P(4-Me-C_6H_4)$_3$ [b]		8.7		234.8	111.7	216
51	P(2-Me-C_6H_4)$_3$ [b]		7.8		230.7	111.7	277
52	P(3-MeO-C_6H_4)$_3$ [b]	7.25	7.7		234.6	111.5	229
53	P[3,5-(MeO)$_2$-C_6H_3]$_3$ [b]	7.19	7.7		237.9	111.5	233

[a] from paper III; [b] from paper I; [c] from paper II.

No	Compound	pK_{aH}(MeCN) experimental	COSMO-RS	SMD	GB [kcal·mol^{-1}]	θ_{CPC} [º]	θ_{H} [º]
54	PPh_3 [b]	7.62	7.1		228.6	111.6	218
55	$P(1\text{-Napht})Ph_2$ [b]	7.29	7.0		230.0	111.6	229
56	$P(4\text{-F-}C_6H_4)_3$ [b]		6.7		224.0	111.6	216
57	$P(1\text{-Napht})_3$ [b]	6.55	6.3		232.3	111.6	247
58	$P(2\text{-F-}C_6H_4)Ph_2$ [b,c]	6.11	5.9	6.3	221.1	110.8	220
59	$P(2,6\text{-}F_2\text{-}C_6H_3)Ph_2$ [b,c]	5.17	5.5		220.7	111.4	221
60	$P(4\text{-Cl-}C_6H_4)_3$ [b]		4.9		223.3	111.4	215
61	PPh_2H [b]		4.7		216.7	110.8	187
62	$P(2\text{-F-}C_6H_4)_2Ph$ [b,c]	4.56	4.5	4.6	219.4	110.5	226
63	$P(2\text{-F-}C_6H_4)_3$ [b]	3.01	3.0		224.1	110.7	231
64	$P(C_6F_5)Ph_2$ [b,c]	2.54	2.7	2.7	212.7	111.6	222
65	$P(2,6\text{-}F_2\text{-}C_6H_3)_2Ph$ [b,c]	2.50	2.5	2.4	217.0	111.7	232
66	$P(2,6\text{-}Cl_2\text{-}C_6H_3)_3$ [b]	1.70	1.7		225.5	115.4	277
67	$P(CF_3)Me_2$		1.7	3.8	196.5	109.8	169
68	$P(2,6\text{-}F_2\text{-}C_6H_3)_3$ [b]		0.5		222.0	113.5	255
69	$P[CH_2CH(CF_3)_2]_3$ [b]		0		201.9	109.0	256
70	PPh_2Cl [b]		−0.2		212.5	111.0	202
71	$P(C_6F_5)_2Ph$ [b]		−2		211.1	112.3	234
72	$P[3,5\text{-}(CF_3)_2\text{-}C_6H_3]_3$ [b]		−2		200.5	111.4	221
73	$P(CH_2CF_3)_3$ [b]		−3		194.6	111.1	228
74	$P(C_6F_5)_3$ [b,c]		−7	−8	190.4	112.6	256
75	$P(CF_3)_2Me$ [c]		−13	−11	174.4	109.0	174
76	PF_3 [c]		−23	−24	146.2	108.0	149
77	$P(CF_3)_3$ [c]		−27	−25	156.4	109.0	185
78	$P(C_2F_5)_3$ [c]		−27	−29	158.8	109.0	217
79	$P(C_3F_7)_3$ [c]		−27	−28	162.1	110.2	227
80	$P(C_4F_9)_3$ [c]		−28	−32	159.8	110.3	215

[a] from paper III; [b] from paper I; [c] from paper II.

3.1.1. General trends in phosphane basicity

The impact of electron-donating and -withdrawing substituents on phosphane basicity is illustrated in Scheme 8.

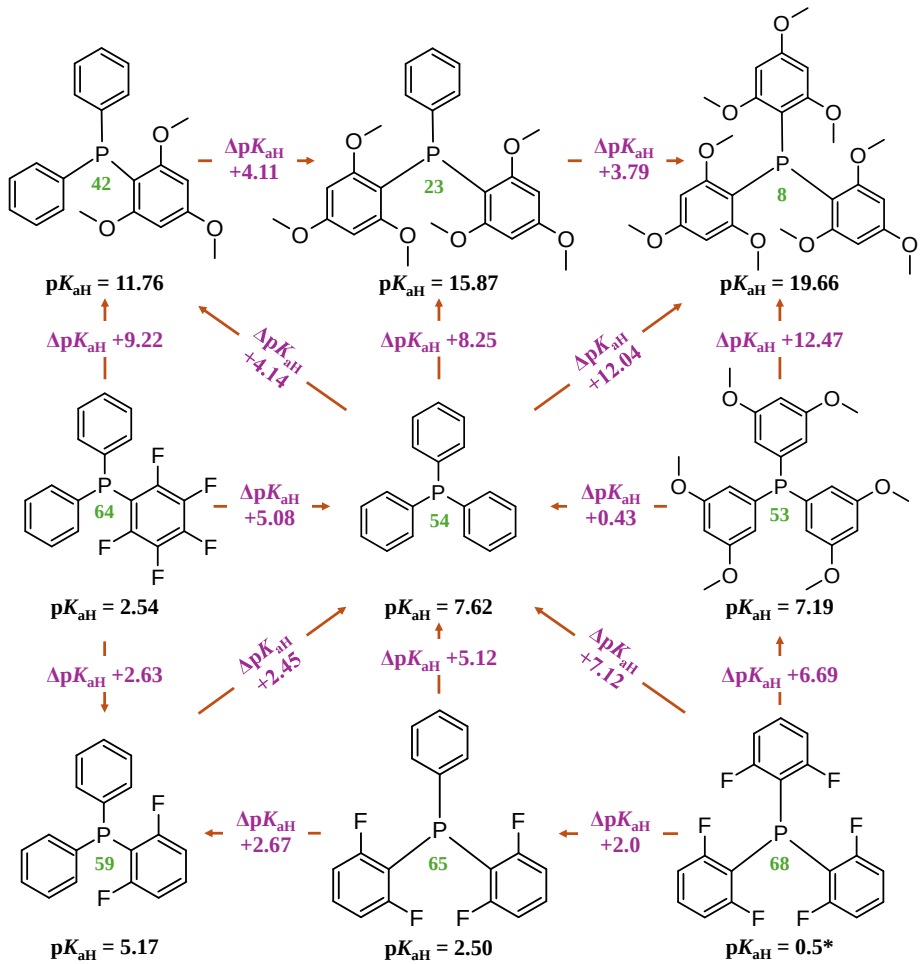

Scheme 8. Substituent impact on phosphane basicity. pK_{aH}(MeCN) values are from Table 1, corresponding compound numbers are marked in green below the structures. * Computational COSMO-RS value.

Methoxy groups in the ortho and para positions enhance the basicity of aromatic phosphanes, whereas they reduce it in the meta position (where resonance effects are absent) since they also act as inductive electron-withdrawing substituents (inductive substituent constant σ_F(MeO) = 0.30; for comparison, $\sigma_F(NH_2) = 0.09$)[78] to some extent. The increase in basicity induced by electron-donating substituents in ortho/para positions is primarily due to stabilization of the protonated phosphane through resonance effects (resonance substituent

constant σ_R(MeO) = −0.43),[78] as these groups reduce the positive charge density on the phosphorus atom, making protonation more favourable. Additionally, methoxy groups in the ortho position offer further stabilization of the protonated form through charge-charge interaction due to the spatial proximity of the oxygen atoms to the proton attached to the P atom.

Although the lone pair on phosphorus is only weakly conjugated with the aromatic rings due to suboptimal orbital alignment, a minor resonance effect remains.[79] As a result, electron-donating substituents can enhance the accessibility of the phosphorus lone pair, further contributing to increased basicity.

On the other hand, groups with resonance-accepting character like NO_2 (σ_R = 0.16)[78] in the ortho/para position, as well as strong inductive electron-withdrawing groups like NO_2 (σ_F = 0.64),[78] F (σ_F = 0.57),[78] and CF_3 (σ_F = 0.46)[78] in any position, lead to a decrease in the basicity of aromatic phosphanes. Electron-accepting groups reduce basicity by destabilizing the protonated form and decreasing the availability of the phosphorus lone pair.

Alkyl-substituted phosphanes typically display higher basicity than their aromatic counterparts. This trend is largely due to the negative field-inductive effect of the phenyl ring (σ_F = 0.14),[78] which destabilizes the protonated species. Similarly, fluorination of alkyl groups decreases phosphane basicity owing to the strong electron-withdrawing character of fluorine. Replacing a methyl group with a trifluoromethyl group in PMe_3 results in a decrease in basicity by approximately 11–15 pK_{aH} units per methyl group (Scheme 9). This very large change underscores the unique characteristics of fluorine, arising from its notably high electronegativity.

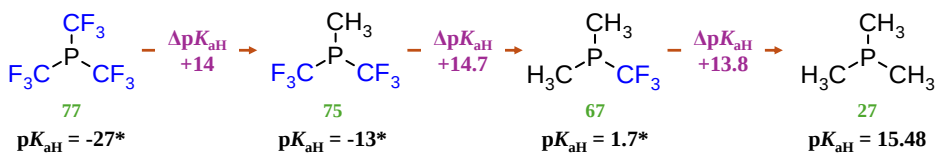

Scheme 9. The impact of replacing CH_3 groups with CF_3 on phosphane basicity. pK_{aH}(MeCN) values are from Table 1, corresponding compound numbers are marked in green below the structures. * Computational COSMO-RS values.

3.1.2. Perfluoroalkylphosphanes

Perfluoroalkyl groups (Rf) are inductive electron-withdrawing substituents ($\sigma_F(CF_3)$ = 0.46); for comparison, $\sigma_F(CH_3)$ = −0.01)[78] and, when at least one fluorine atom is in the alpha position, also act as resonance acceptors ($\sigma_R(CF_3)$ = 0.09; for comparison, $\sigma_R(CH_3)$ = −0.13)[78] through anionic hyperconjugation.

As a result of their pronounced electron-withdrawing nature, Rf groups significantly reduce the basicity of phosphanes. Although the uncertainty of their computational pK_{aH} values likely spans several units, the results of this work indicate that the pK_{aH} values of $P(CF_3)_3$ (**77**), $P(C_2F_5)_3$ (**78**), $P(C_3F_7)_3$ (**79**), and

$P(C_4F_9)_3$ (**80**) are all below −20. This clearly demonstrates that $P(Rf)_3$ compounds possess negligible basicity and cannot be considered Brønsted-Lowry bases under almost any realistic experimental conditions. However, owing to the strong π-backbonding effect induced by the highly electronegative substituents, these compounds display markedly greater π-acidity compared to conventional PR_3 phosphanes. This increased π-acidity arises from the lower energy of their σ* anti-bonding orbitals, an effect that contributes significantly to the stabilization of the resulting transition metal complexes.[80,81]

3.1.3. Phosphazenes

The impact of different substituents on phosphazene basicity is illustrated in Scheme 10.

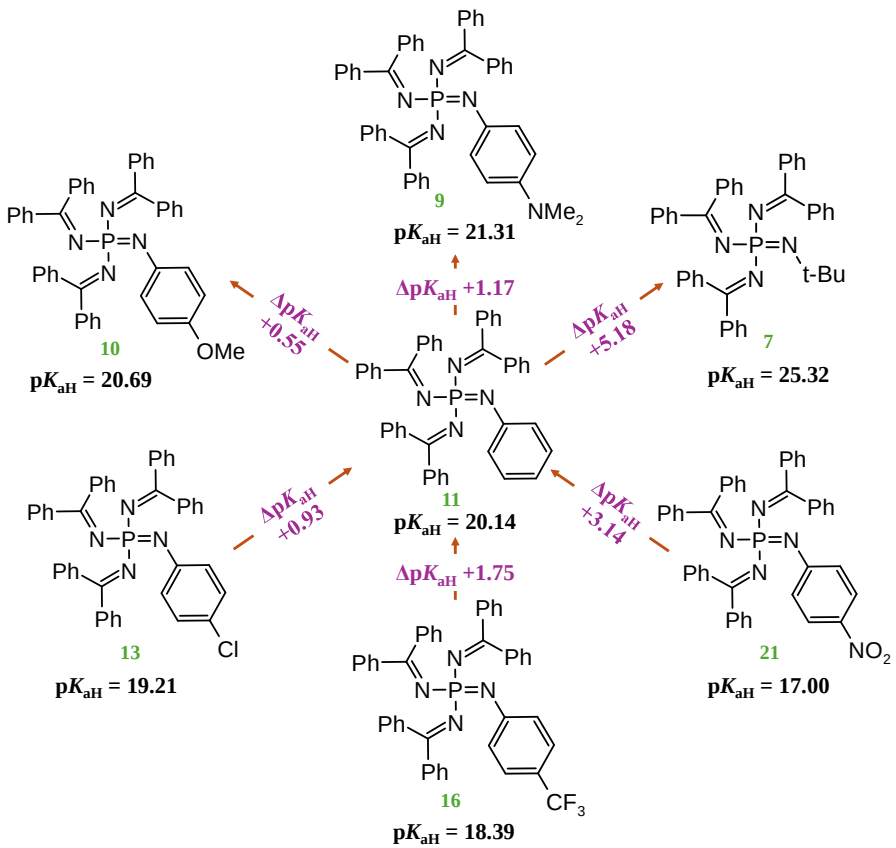

Scheme 10. Substituent impact on phosphazene basicity. pK_{aH}(MeCN) values are from Table 1. The corresponding compound numbers are marked in green below the structures.

Aryl-imino phosphazenes exhibit stabilization of their neutral forms through delocalization of the electrons on the nitrogen – the main protonation site – into the aromatic ring.[82] This delocalization, which reduces the availability of the

nitrogen lone pair for protonation, is absent in alkyl-imino phosphazenes. Instead, in the latter, the positive charge generated upon protonation is stabilized via inductive effects of the alkyl groups. This results in significantly higher basicity of alkyl-imino phosphazenes compared to their aryl-imino counterparts.

Furthermore, aryl-imino phosphazenes bearing electron-donating substituents groups (e.g., NMe_2 and MeO) in para position show enhanced basicity relative to the unsubstituted analogue. This is due to the increased ability of these donor groups to delocalize the positive charge on nitrogen formed upon protonation, thereby stabilizing the conjugate acid. Conversely, the presence of electron-withdrawing substituents (e.g., Cl, CF_3, and NO_2) decreases the basicity of the respective phosphazenes by destabilizing the protonated form through increasing the positive charge on the nitrogen.

3.2. Electronic and steric properties of phosphanes

The TEP value mentioned in the Literature overview is widely used to characterize the electronic properties of phosphanes.[83] However, it is not a convenient tool for rapid comparison of phosphanes. Determination of the TEP value necessitates the preparation or calculation of a ligand-$Ni(CO)_3$ complex. This poses practical challenges, as the starting material, $Ni(CO)_4$, is a toxic gas that is not readily available in most research laboratories, and the calculation of complexes with the involvement of transition metals can be resource-intensive. Moreover, the results are highly sensitive to solvent effects,[2] making computational gas-phase values less reliable without a suitable reference system.

As an alternative, the pK_{aH} value can be employed to characterize the electronic properties of phosphanes. pK_{aH} values can be directly measured from a free phosphane or calculated using the structures of the neutral and protonated forms. pK_{aH} values offer valuable insights into the electronic properties of compounds and are generally not significantly impacted by steric hindrance from distant substituents. However, substituents located near the protonation site can sometimes markedly affect both the stability of the protonated form and the accessibility of the proton. Nevertheless, as demonstrated in paper I, pK_{aH} values showed a strong correlation with TEP values for the available dataset, with only a few notable outliers. For more details, the reader is referred to paper I.

Another important property of a ligand is its size. Similar to the TEP value, the Tolman cone angle and other modern steric parameters are derived from metal-ligand complexes.[3,84] Although these parameters offer higher precision in absolute terms, they are often impractical for quick ligand comparisons. As a more efficient alternative, θ_{CPC} and θ_H angles,[5] which are obtained directly from protonated ligand structures, present a valuable option for preliminary screening and can significantly reduce resource demands.

The C–P–C bond angle provides one of the simplest and most accessible estimates of ligand size, easily derived from computational structures or crystallographic data. However, this descriptor has limitations, particularly for branched

phosphanes, where the C–P–C angle is not affected as much by the rest of the substituent structure. In such cases, the θ_H angle offers a more reliable approach, showing reasonable correlation with the Tolman cone angle. Further details on these parameters can be found in paper I.

3.3. Benzophenoneimino compounds

Since phosphanes bearing imino substituents ($P(N{=}CR_2)_3$) are electron-rich nucleophiles, many of which exhibit remarkable basicity,[7,85] benzophenoneimino (bpi, $Ph_2C{=}N–$) substituted phosphane and its phosphazene derivatives were synthesized. The incorporation of the bpi group provides the resulting phosphazenes with excellent UV-Vis spectral properties, making them particularly suitable for spectrophotometric pK_{aH} measurements. As a result, they contribute to the supplementation of previously established UV-Vis basicity scales.[4,42]

However, the pK_{aH} measurement of the starting compound $P(bpi)_3$ was unsuccessful due to its high reactivity toward nucleophiles, including the anions of commonly used acidic titrants. It was also observed that upon adding bis(trifluoromethanesulfonyl)amine (Tf_2NH) to the phosphane, $P(bpi)_3$ undergoes a reaction to form a heterocyclic cation via the formation of a phosphinophosphonium cation $[P_2(bpi)_5]^+$ as the intermediate (Scheme 11). These findings indicate that under used conditions $P(bpi)_3$ does not behave as a Brønsted-Lowry base.

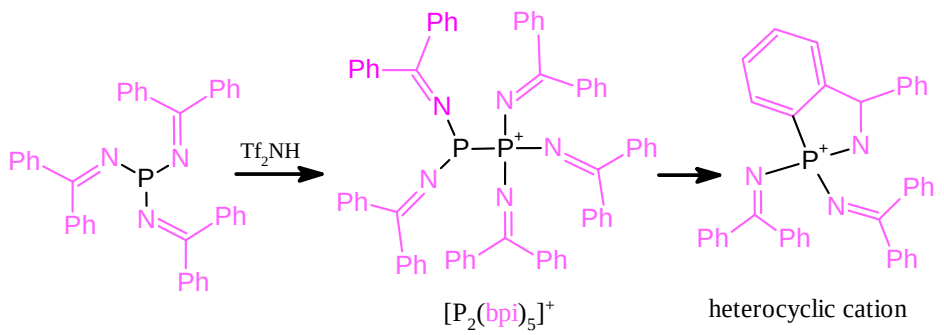

Scheme 11. Formation of a heterocyclic cation as a result of adding acid to $P(bpi)_3$.

Cyclization was also observed during the deprotonation of some phosphonium cations. In most cases, deprotonation led to mixtures of decomposition products and these compounds were not investigated further. However, the deprotonation of $(bpi)_3P^+–CH_2Ph$ resulted in the formation of a P–N heterocyclic compound (Scheme 7) as the main product. Compounds featuring adjacent phosphorus and nitrogen atoms, and P=C double bonds are relatively rare, with only a few examples of such heterocycles reported in the literature.[86–90] Indirect evidence based on UV-Vis spectroscopy suggests that deprotonation of $(bpi)_3P^+–CH_3$ and $(bpi)_3P^+–CH_2CH_3$ leads to the formation of P–N heterocycles as well.

When employed as a substituent in organophosphorus compounds, the benzophenoneimino group appears to exhibit peculiar behavior, frequently leading to cyclization at the ortho position of one of the phenyl rings. Nevertheless, the bpi-phosphazenes seem to be stable and valuable bases with unexplored potential application as reagents in organic chemistry. The reactions and properties of bpi-compounds are described in more detail in paper III.

SUMMARY

The aim of this thesis was to compile basicity data of phosphanes dispersed across various sources into a unified and comprehensive overview, while also addressing notable gaps in the existing dataset. An additional objective was to explore simpler alternatives to the commonly used descriptors for characterizing phosphanes. Furthermore, the synthesis of new bases with relatively high basicity and favorable UV-Vis properties was pursued, with the goal of supplementing the UV-Vis spectrophotometric basicity scale in acetonitrile.

pK_{aH} values for a structurally diverse range of phosphanes were presented, including both newly measured or calculated values and data compiled from the literature. As shown in this thesis, phosphane basicity can be systematically adjusted through substituent modification, spanning a wide pK_{aH} range from roughly −30 to beyond 30 (in acetonitrile). Substituents with electron-withdrawing properties tend to lower the pK_{aH} value, thus reducing the basicity of phosphanes, whereas electron-donating groups elevate it.

A framework for assessing the properties of phosphanes is proposed in this thesis. Based on the observed correlation between pK_{aH} values and conventional Tolman Electronic Parameters (TEP), it is suggested that pK_{aH} values could serve as a practical alternative to TEP values for evaluating electronic characteristics of phosphanes. Additionally, new steric descriptors for describing the steric properties of phosphanes were presented as alternatives to the widely used Tolman cone angle, which, despite its prevalence, is relatively challenging to obtain. For preliminary screening purposes, C–P–C angles (θ_{CPC}) or the exact cone angles of protonated phosphanes (θ_H), depending on the specific set of compounds, may be used. The use of these values has the potential to simplify future ligand screening processes, eliminating the need for computational modeling or experimental preparation of metal-ligand complexes.

Novel phosphazene bases derived from benzophenoneimino (bpi) substituted phosphane were synthesized with experimental pK_{aH} values ranging from 17 to 26 in acetonitrile. Although these bpi-phosphazenes are in terms of basicity outperformed by many existing bases, they still exhibit considerable basic strength and could offer practical advantages as reagents.

In contrast to the bpi-phosphazenes demonstrating reasonable stability, the protonation of P(bpi)$_3$ resulted in the formation of a unique P-N heterocycle. Similar phenomenon was observed when bpi-substituted phosphonium cations were deprotonated. This indicates high steric crowding and instability of these specific compounds.

In conclusion, the objectives of this thesis were successfully achieved, resulting in the provision of basicity data and steric characterization for 63 phosphanes. Furthermore, 15 novel bpi-compounds were prepared and characterized, including 9 new bases for which experimental pK_{aH} values were obtained. Basicity data was also provided for their starting materials.

REFERENCES

(1) Pignolet, L. M. *Homogeneous Catalysis with Metal Phosphine Complexes*; Springer Science & Business Media, 2013.

(2) Tolman, C. A. Electron Donor-Acceptor Properties of Phosphorus Ligands. Substituent Additivity. *J. Am. Chem. Soc.* **1970**, *92* (10), 2953–2956. https://doi.org/10.1021/ja00713a006.

(3) Tolman, C. A. Steric Effects of Phosphorus Ligands in Organometallic Chemistry and Homogeneous Catalysis. *Chem. Rev.* **1977**, *77* (3), 313–348. https://doi.org/10.1021/cr60307a002.

(4) Tshepelevitsh, S.; Kütt, A.; Lõkov, M.; Kaljurand, I.; Saame, J.; Heering, A.; Plieger, P. G.; Vianello, R.; Leito, I. On the Basicity of Organic Bases in Different Media. *Eur. J. Org. Chem.* **2019**, *2019* (40), 6735–6748. https://doi.org/10.1002/ejoc.201900956.

(5) Pikma, M.-L.; Tshepelevitsh, S.; Selberg, S.; Kaljurand, I.; Leito, I.; Kütt, A. pK_{aH} Values and θ_H Angles of Phosphanes to Predict Their Electronic and Steric Parameters. *Dalton Trans.* **2024**, *53* (34), 14226–14236. https://doi.org/10.1039/D4DT01430H.

(6) Haav, K.; Saame, J.; Kütt, A.; Leito, I. Basicity of Phosphanes and Diphosphanes in Acetonitrile. *Eur. J. Org. Chem.* **2012**, *2012* (11), 2167–2172. https://doi.org/10.1002/ejoc.201200009.

(7) Mehlmann, P.; Mück-Lichtenfeld, C.; Tan, T. T. Y.; Dielmann, F. Tris(Imidazolin-2-Ylidenamino)Phosphine: A Crystalline Phosphorus(III) Superbase That Splits Carbon Dioxide. *Chem. Eur. J.* **2017**, *23* (25), 5929–5933. https://doi.org/10.1002/chem.201604971.

(8) Greb, L.; Tussing, S.; Schirmer, B.; Oña-Burgos, P.; Kaupmees, K.; Lõkov, M.; Leito, I.; Grimme, S.; Paradies, J. Electronic Effects of Triarylphosphines in Metal-Free Hydrogen Activation: A Kinetic and Computational Study. *Chem. Sci.* **2013**, *4* (7), 2788–2796. https://doi.org/10.1039/C3SC50347J.

(9) Saame, J.; Rodima, T.; Tshepelevitsh, S.; Kütt, A.; Kaljurand, I.; Haljasorg, T.; Koppel, I. A.; Leito, I. Experimental Basicities of Superbasic Phosphonium Ylides and Phosphazenes. *J. Org. Chem.* **2016**, *81* (17), 7349–7361. https://doi.org/10.1021/acs.joc.6b00872.

(10) Crabtree, R. H. Carbonyls, Phosphine Complexes, and Ligand Substitution Reactions. In *The Organometallic Chemistry of the Transition Metals*; John Wiley & Sons, Ltd, 2005; pp 87–124. https://doi.org/10.1002/0471718769.ch4.

(11) Orpen, A. G.; Connelly, N. G. Structural Systematics: The Role of P-A σ* Orbitals in Metal-Phosphorus π-Bonding in Redox-Related Pairs of M-PA_3 Complexes (A = R, Ar, OR; R = Alkyl). *Organometallics* **1990**, *9* (4), 1206–1210. https://doi.org/10.1021/om00118a048.

(12) Brisdon, A. K.; Herbert, C. J. Fluoroalkyl-Containing Phosphines. *Coord Chem. Rev.* **2013**, *257* (5), 880–901. https://doi.org/10.1016/j.ccr.2012.07.028.

(13) Gilheany, D. G. Structure and Bonding in Organophosphorus(III) Compounds. In *Organophosphorus Compounds (1990)*; John Wiley & Sons, Ltd: Chichester, U.K, 1990; pp 9–49. https://doi.org/10.1002/9780470034439.ch2.

(14) Levason, W. Phosphine Complexes of Transition Metals. In *Organophosphorus Compounds (1990)*; John Wiley & Sons, Ltd: Chichester, U.K, 1990; pp 567–641. https://doi.org/10.1002/9780470034439.ch15.

(15) Hudson, H. R. Acid–Base and Hydrogen-Bonding Properties of Phosphines. In *Organophosphorus Chemistry*; John Wiley & Sons, Ltd: Chichester, U.K, 1990; pp 473–487. https://doi.org/10.1002/9780470034439.ch12.
(16) Hartley, F. R. Introduction. In *Organophosphorus Compounds (1990)*; John Wiley & Sons, Ltd, 1990; pp 1–8. https://doi.org/10.1002/9780470034439.ch1.
(17) Hudson, H. R. Nucleophilic Reactions of Phosphines. In *Organophosphorus Chemistry*; John Wiley & Sons, Ltd: Chichester, U.K, 1990; pp 385–471. https://doi.org/10.1002/9780470034439.ch11.
(18) Elie, B. T.; Levine, C.; Ubarretxena-Belandia, I.; Varela-Ramírez, A.; Aguilera, R. J.; Ovalle, R.; Contel, M. Water-Soluble (Phosphane)Gold(I) Complexes – Applications as Recyclable Catalysts in a Three-Component Coupling Reaction and as Antimicrobial and Anticancer Agents. *Eur. J. Inorg. Chem.* **2009**, *2009* (23), 3421–3430. https://doi.org/10.1002/ejic.200900279.
(19) Broggi, J.; Urbina-Blanco, C. A.; Clavier, H.; Leitgeb, A.; Slugovc, C.; Slawin, A. M. Z.; Nolan, S. P. The Influence of Phosphane Ligands on the Versatility of Ruthenium–Indenylidene Complexes in Metathesis. *Chem. Eur. J.* **2010**, *16* (30), 9215–9225. https://doi.org/10.1002/chem.201000659.
(20) Amoroso, D.; Snelgrove, J. L.; Conrad, J. C.; Drouin, S. D.; Yap, G. P. A.; Fogg, D. E. An Attractive Route to Olefin Metathesis Catalysts: Facile Synthesis of a Ruthenium Alkylidene Complex Containing Labile Phosphane Donors. *Adv. Synth. Catal.* **2002**, *344* (6–7), 757–763. https://doi.org/10.1002/1615-4169(200208)344:6/7<757::AID-ADSC757>3.0.CO;2-X.
(21) Findeis, R. A.; Gade, L. H. Tripodal Phosphane Ligands with Novel Linker Units and Their Rhodium Complexes as Building Blocks for Dendrimer Catalysts. *Eur. J. Inorg. Chem.* **2003**, *2003* (1), 99–110. https://doi.org/10.1002/ejic.200390019.
(22) Sanford, M. S.; Love, J. A. Mechanism of Ruthenium-Catalyzed Olefin Metathesis Reactions. In *Handbook of Metathesis*; John Wiley & Sons, Ltd, 2003; pp 112–131. https://doi.org/10.1002/9783527619481.ch9.
(23) Welch, G. C.; Juan, R. R. S.; Masuda, J. D.; Stephan, D. W. Reversible, Metal-Free Hydrogen Activation. *Science* **2006**, *314*, 1124–1127.
(24) Stephan, D. W. Catalysis, FLPs, and Beyond. *Chem* **2020**, *6* (7), 1520–1526. https://doi.org/10.1016/j.chempr.2020.05.007.
(25) Methot, J. L.; Roush, W. R. Nucleophilic Phosphine Organocatalysis. *Adv. Synth. Catal.* **2004**, *346* (9-10), 1035–1050. https://doi.org/10.1002/adsc.200404087.
(26) Gilheany, D. G.; Mitchell, C. M. Preparation of Phosphines. In *Organophosphorus Compounds (1990)*; John Wiley & Sons, Ltd: Chichester, U.K, 1990; pp 151–190. https://doi.org/10.1002/9780470034439.ch7.
(27) Wauters, I.; Debrouwer, W.; Stevens, C. V. Preparation of Phosphines through C-P Bond Formation. *Beilstein J. Org. Chem.* **2014**, *10*, 1064–1096. https://doi.org/10.3762/bjoc.10.106.
(28) Kaljurand, I.; Rodima, T.; Leito, I.; Koppel, I. A.; Schwesinger, R. Self-Consistent Spectrophotometric Basicity Scale in Acetonitrile Covering the Range between Pyridine and DBU. *J. Org. Chem.* **2000**, *65* (19), 6202–6208. https://doi.org/10.1021/jo005521j.
(29) Bachrach, S. M.; Nitsche, C. I. Structure, Bonding and Spectroscopic Properties of Phosphonium Ylides. In *Organophosphorus Compounds (1993)*; John Wiley & Sons, Ltd, 1993; pp 273–302. https://doi.org/10.1002/047003436X.ch4.

(30) Gilheany, D. G. Structure and Bonding in Phosphonium Ylides, Salts and Phosphoranes. In *Organophosphorus Compounds (1993)*; John Wiley & Sons, Ltd, 1993; pp 1–44. https://doi.org/10.1002/047003436X.ch1.
(31) Schwesinger, R.; Schlemper, H. Peralkylated Polyaminophosphazenes— Extremely Strong, Neutral Nitrogen Bases. *Angew. Chem. Int. Ed. Engl.* **1987**, *26* (11), 1167–1169. https://doi.org/10.1002/anie.198711671.
(32) Schwesinger, R.; Hasenfratz, C.; Schlemper, H.; Walz, L.; Peters, E.-M; Peters, K.; von Schnering, H. G. How Strong and How Hindered Can Uncharged Phosphazene Bases Be? *Angew. Chem. Int. Ed. Engl.* **1993**, *32* (9), 1361–1363. https://doi.org/10.1002/anie.199313611.
(33) Kolomeitsev, A. A.; Koppel, I. A.; Rodima, T.; Barten, J.; Lork, E.; Röschenthaler, G.-V.; Kaljurand, I.; Kütt, A.; Koppel, I.; Mäemets, V.; Leito, I. Guanidinophosphazenes: Design, Synthesis, and Basicity in THF and in the Gas Phase. *J. Am. Chem. Soc.* **2005**, *127* (50), 17656–17666. https://doi.org/10.1021/ja053543n.
(34) Rossi, R. D. What Does the Acid Ionization Constant Tell You? An Organic Chemistry Student Guide. *J. Chem. Educ.* **2013**, *90* (2), 183–190. https://doi.org/10.1021/ed200512n.
(35) Hunter, E. P. L.; Lias, S. G. Evaluated Gas Phase Basicities and Proton Affinities of Molecules: An Update. *J. Phys. Chem. Ref. Data* **1998**, *27* (3), 413–656. https://doi.org/10.1063/1.556018.
(36) Reichardt, C.; Welton, T. *Solvents and Solvent Effects in Organic Chemistry*; John Wiley & Sons, 2010.
(37) Perrin, C. L.; Agranat, I.; Bagno, A.; Braslavsky, S. E.; Fernandes, P. A.; Gal, J.-F.; Lloyd-Jones, G. C.; Mayr, H.; Murdoch, J. R.; Nudelman, N. S.; Radom, L.; Rappoport, Z.; Ruasse, M.-F.; Siehl, H.-U.; Takeuchi, Y.; Tidwell, T. T.; Uggerud, E.; Williams, I. H. Glossary of Terms Used in Physical Organic Chemistry (IUPAC Recommendations 2021). *Pure Appl. Chem.* **2022**, *94* (4), 353–534. https://doi.org/10.1515/pac-2018-1010.
(38) Izutsu, K. *Electrochemistry in Nonaqueous Solutions*; John Wiley & Sons, 2009.
(39) Kütt, A.; Selberg, S.; Kaljurand, I.; Tshepelevitsh, S.; Heering, A.; Darnell, A.; Kaupmees, K.; Piirsalu, M.; Leito, I. pK_a Values in Organic Chemistry – Making Maximum Use of the Available Data. *Tetrahedron Lett.* **2018**, *59* (42), 3738–3748. https://doi.org/10.1016/j.tetlet.2018.08.054.
(40) Kaljurand, I.; Kütt, A.; Sooväli, L.; Rodima, T.; Mäemets, V.; Leito, I.; Koppel, I. A. Extension of the Self-Consistent Spectrophotometric Basicity Scale in Acetonitrile to a Full Span of 28 pK_a Units: Unification of Different Basicity Scales. *J. Org. Chem.* **2005**, *70* (3), 1019–1028. https://doi.org/10.1021/jo048252w.
(41) Pikma, M.-L.; Lõkov, M.; Tshepelevitsh, S.; Saame, J.; Haljasorg, T.; Toom, L.; Selberg, S.; Leito, I.; Kütt, A. Tris(Benzophenoneimino)Phosphane and Related Compounds. *Eur. J. Org. Chem.* **2023**, *26* (28), e202300453. https://doi.org/10.1002/ejoc.202300453.
(42) Lõkov, M.; Kesküla, C.; Tshepelevitsh, S.; Pikma, M.-L.; Saame, J.; Trubitsõn, D.; Kanger, T.; Leito, I. The Acidity of Weak NH Acids: Expanding the pK_a Scale in Acetonitrile. *ACS Org. Inorg. Au* **2025**, *5* (2), 144–155. https://doi.org/10.1021/acsorginorgau.4c00095.
(43) Parman, E.; Toom, L.; Selberg, S.; Leito, I. Determination of pK_a Values of Fluorocompounds in Water Using ^{19}F NMR. *J. Phys. Org. Chem.* **2019**, *32* (6), e3940. https://doi.org/10.1002/poc.3940.

(44) Parman, E.; Lõkov, M.; Järviste, R.; Tshepelevitsh, S.; Semenov, N. A.; Chulanova, E. A.; Salnikov, G. E.; Prima, D. O.; Slizhov, Y. G.; Leito, I.; Zibarev, A. V. Acid-Base and Anion Binding Properties of Tetrafluorinated 1,3-Benzodiazole, 1,2,3-Benzotriazole and 2,1,3-Benzoselenadiazole. *ChemPhysChem* **2021**, *22* (22), 2329–2335. https://doi.org/10.1002/cphc.202100475.
(45) Trummal, A.; Rummel, A.; Lippmaa, E.; Koppel, I.; Koppel, I. A. Calculations of pK_a of Superacids in 1,2-Dichloroethane. *J Phys Chem A* **2011**, *115* (24), 6641–6645. https://doi.org/10.1021/jp202434p.
(46) Kaupmees, K.; Trummal, A.; Leito, I. Basicities of Strong Bases in Water: A Computational Study. *Croat. Chem. Acta* **2014**, *87* (4), 385–395. https://doi.org/10.5562/cca2472.
(47) Li, J.-N.; Fu, Y.; Liu, L.; Guo, Q.-X. First-Principle Predictions of Basicity of Organic Amines and Phosphines in Acetonitrile. *Tetrahedron* **2006**, *62* (50), 11801–11813. https://doi.org/10.1016/j.tet.2006.09.018.
(48) Ding, F.; Smith, J. M.; Wang, H. First-Principles Calculation of pK_a Values for Organic Acids in Nonaqueous Solution. *J. Org. Chem.* **2009**, *74* (7), 2679–2691. https://doi.org/10.1021/jo802641r.
(49) Hohenberg, P.; Kohn, W. Inhomogeneous Electron Gas. *Phys. Rev.* **1964**, *136* (3B), B864–B871. https://doi.org/10.1103/PhysRev.136.B864.
(50) Orio, M.; Pantazis, D. A.; Neese, F. Density Functional Theory. *Photosynth. Res.* **2009**, *102* (2), 443–453. https://doi.org/10.1007/s11120-009-9404-8.
(51) Koch, W.; Holthausen, M. C. *A Chemist's Guide to Density Functional Theory*; John Wiley & Sons, 2015.
(52) Parr, R. G. Density Functional Theory of Atoms and Molecules. In *Horizons of Quantum Chemistry*; Fukui, K., Pullman, B., Eds.; Springer Netherlands: Dordrecht, 1980; pp 5–15. https://doi.org/10.1007/978-94-009-9027-2_2.
(53) Feller, D.; Davidson, E. R. Basis Sets for Ab Initio Molecular Orbital Calculations and Intermolecular Interactions. In *Reviews in Computational Chemistry*; John Wiley & Sons, Ltd, 1990; pp 1–43. https://doi.org/10.1002/9780470125786.ch1.
(54) Davidson, E. R.; Feller, D. Basis Set Selection for Molecular Calculations. *Chem. Rev.* **1986**, *86* (4), 681–696. https://doi.org/10.1021/cr00074a002.
(55) Pitman, S. J.; Evans, A. K.; Ireland, R. T.; Lempriere, F.; McKemmish, L. K. Benchmarking Basis Sets for Density Functional Theory Thermochemistry Calculations: Why Unpolarized Basis Sets and the Polarized 6-311G Family Should Be Avoided. *J. Phys. Chem. A* **2023**, *127* (48), 10295–10306. https://doi.org/10.1021/acs.jpca.3c05573.
(56) Tomasi, J.; Mennucci, B.; Cammi, R. Quantum Mechanical Continuum Solvation Models. *Chem. Rev.* **2005**, *105* (8), 2999–3094. https://doi.org/10.1021/cr9904009.
(57) Barone, V.; Cossi, M. Quantum Calculation of Molecular Energies and Energy Gradients in Solution by a Conductor Solvent Model. *J. Phys. Chem. A* **1998**, *102* (11), 1995–2001. https://doi.org/10.1021/jp9716997.
(58) Cossi, M.; Rega, N.; Scalmani, G.; Barone, V. Energies, Structures, and Electronic Properties of Molecules in Solution with the C-PCM Solvation Model. *J. Comput. Chem.* **2003**, *24* (6), 669–681. https://doi.org/10.1002/jcc.10189.
(59) Foresman, J. B.; Keith, T. A.; Wiberg, K. B.; Snoonian, J.; Frisch, M. J. Solvent Effects. 5. Influence of Cavity Shape, Truncation of Electrostatics, and Electron Correlation on Ab Initio Reaction Field Calculations. *J. Phys. Chem.* **1996**, *100* (40), 16098–16104. https://doi.org/10.1021/jp960488j.

(60) Cancès, E.; Mennucci, B.; Tomasi, J. A New Integral Equation Formalism for the Polarizable Continuum Model: Theoretical Background and Applications to Isotropic and Anisotropic Dielectrics. *J. Chem. Phys.* **1997**, *107* (8), 3032–3041. https://doi.org/10.1063/1.474659.
(61) Mennucci, B.; Tomasi, J. Continuum Solvation Models: A New Approach to the Problem of Solute's Charge Distribution and Cavity Boundaries. *J. Chem. Phys.* **1997**, *106* (12), 5151–5158. https://doi.org/10.1063/1.473558.
(62) Mennucci, B.; Cancès, E.; Tomasi, J. Evaluation of Solvent Effects in Isotropic and Anisotropic Dielectrics and in Ionic Solutions with a Unified Integral Equation Method: Theoretical Bases, Computational Implementation, and Numerical Applications. *J. Phys. Chem. B* **1997**, *101* (49), 10506–10517. https://doi.org/10.1021/jp971959k.
(63) Tomasi, J.; Mennucci, B.; Cancès, E. The IEF Version of the PCM Solvation Method: An Overview of a New Method Addressed to Study Molecular Solutes at the QM Ab Initio Level. *J. Mol. Struct. THEOCHEM* **1999**, *464* (1), 211–226. https://doi.org/10.1016/S0166-1280(98)00553-3.
(64) Marenich, A. V.; Cramer, C. J.; Truhlar, D. G. Universal Solvation Model Based on Solute Electron Density and on a Continuum Model of the Solvent Defined by the Bulk Dielectric Constant and Atomic Surface Tensions. *J. Phys. Chem. B* **2009**, *113* (18), 6378–6396. https://doi.org/10.1021/jp810292n.
(65) Marenich, A. V.; Olson, R. M.; Kelly, C. P.; Cramer, C. J.; Truhlar, D. G. Self-Consistent Reaction Field Model for Aqueous and Nonaqueous Solutions Based on Accurate Polarized Partial Charges. *J. Chem. Theory Comput.* **2007**, *3* (6), 2011–2033. https://doi.org/10.1021/ct7001418.
(66) Chipman, D. M. Charge Penetration in Dielectric Models of Solvation. *J. Chem. Phys.* **1997**, *106* (24), 10194–10206. https://doi.org/10.1063/1.474048.
(67) Zhan, C.-G.; Bentley, J.; Chipman, D. M. Volume Polarization in Reaction Field Theory. *J. Chem. Phys.* **1998**, *108* (1), 177–192. https://doi.org/10.1063/1.475371.
(68) Chipman, D. M. New Formulation and Implementation for Volume Polarization in Dielectric Continuum Theory. *J. Chem. Phys.* **2006**, *124* (22), 224111. https://doi.org/10.1063/1.2203068.
(69) Herbert, J. M. Dielectric Continuum Methods for Quantum Chemistry. *WIREs Comput. Mol. Sci.* **2021**, *11* (4), e1519. https://doi.org/10.1002/wcms.1519.
(70) Klamt, A. Conductor-like Screening Model for Real Solvents: A New Approach to the Quantitative Calculation of Solvation Phenomena. *J. Phys. Chem.* **1995**, *99* (7), 2224–2235. https://doi.org/10.1021/j100007a062.
(71) Klamt, A. *COSMO-RS: From Quantum Chemistry to Fluid Phase Thermodynamics and Drug Design*; Elsevier, 2005.
(72) Klamt, A.; Eckert, F.; Arlt, W. COSMO-RS: An Alternative to Simulation for Calculating Thermodynamic Properties of Liquid Mixtures. *Annu. Rev. Chem. Biomol. Eng.* **2010**, *1* (Volume 1, 2010), 101–122. https://doi.org/10.1146/annurev-chembioeng-073009-100903.
(73) Bryant, R. G. The NMR Time Scale. *J. Chem. Educ.* **1983**, *60* (11), 933. https://doi.org/10.1021/ed060p933.
(74) BIOVIA, Dassault Systèmes, COSMOconfX, 2024. http://www.3ds.com.
(75) BIOVIA, Dassault Systèmes, COSMOtherm, 2025. http://www.3ds.com.
(76) Staudinger, H.; Meyer, J. Über Neue Organische Phosphorverbindungen III. Phosphinmethylenderivate Und Phosphinimine. *Helv. Chim. Acta* **1919**, *2* (1), 635–646. https://doi.org/10.1002/hlca.19190020164.

(77) Leffler, J. E.; Temple, R. D. Staudinger Reaction between Triarylphosphines and Azides. Mechanism. *J. Am. Chem. Soc.* **1967**, *89* (20), 5235–5246. https://doi.org/10.1021/ja00996a027.
(78) Hansch, Corwin.; Leo, A.; Taft, R. W. A Survey of Hammett Substituent Constants and Resonance and Field Parameters. *Chem. Rev.* **1991**, *91* (2), 165–195. https://doi.org/10.1021/cr00002a004.
(79) Hartley, F. R. The Chemistry of Organophosphorus Compounds. *PATAIS Chem. Funct. Groups* **1996**, *4*.
(80) Burton, D. J.; Lu, L. Fluorinated Organometallic Compounds. In *Organofluorine Chemistry: Techniques and Synthons*; Chambers, R. D., Ed.; Springer: Berlin, Heidelberg, 1997; pp 45–89. https://doi.org/10.1007/3-540-69197-9_2.
(81) Duan, L.; Nesterov, V.; Runyon, J. W.; Schnakenburg, G.; Iii, A. J. A.; Streubel, R. Synthesis of Stabilized Phosphinidenoid Complexes Using Weakly Coordinating Cations1. *Aust. J. Chem.* **2011**, *64* (12), 1583–1586. https://doi.org/10.1071/CH11325.
(82) Selberg, S.; Rodima, T.; Lõkov, M.; Tshepelevitsh, S.; Haljasorg, T.; Chhabra, S.; Kadam, S. A.; Toom, L.; Vahur, S.; Leito, I. Synthesis and Properties of Highly Lipophilic Phosphazene Bases. *Tetrahedron Lett.* **2017**, *58* (22), 2098–2102. https://doi.org/10.1016/j.tetlet.2017.04.039.
(83) Tonner, R.; Frenking, G. Tolman's Electronic Parameters for Divalent Carbon(0) Compounds. *Organometallics* **2009**, *28* (13), 3901–3905. https://doi.org/10.1021/om900206w.
(84) Bilbrey, J. A.; Kazez, A. H.; Locklin, J.; Allen, W. D. Exact Ligand Cone Angles. *J. Comput. Chem.* **2013**, *34* (14), 1189–1197. https://doi.org/10.1002/jcc.23217.
(85) Buß, F.; Röthel, M. B.; Werra, J. A.; Rotering, P.; Wilm, L. F. B.; Daniliuc, C. G.; Löwe, P.; Dielmann, F. Tris(Tetramethylguanidinyl)Phosphine: The Simplest Non-Ionic Phosphorus Superbase and Strongly Donating Phosphine Ligand. *Chem. Eur. J.* **2022**, *28* (3), e202104021. https://doi.org/10.1002/chem.202104021.
(86) Barluenga, J.; López, F.; Palacios, F. A Simple Synthesis of 3H-Λ5-Phosphole Derivatives from Alkyldiphenylphosphine Imines and Dimethyl Acetylenedicarboxylate. *J. Chem. Soc. Chem. Commun.* **1986**, No. 21, 1574–1575. https://doi.org/10.1039/C39860001574.
(87) Barluenga, J.; López, F.; Palacios, F. A Simple Synthesis of the First 1-2λ5-Benzazaphosphinine Ring. *Tetrahedron Lett.* **1987**, *28* (37), 4327–4328. https://doi.org/10.1016/S0040-4039(00)96499-2.
(88) Campbell, I. G. M.; Way, J. K. 406. Synthesis and Stereochemistry of Heterocyclic Phosphorus Compounds. Part II. Loss of Optical Activity in the Reduction of (+)-2-Carboxy-9-Phenyl-9-Phosphafluorene 9-Oxide. *J. Chem. Soc. Resumed* **1961**, No. 0, 2133–2141. https://doi.org/10.1039/JR9610002133.
(89) Álvarez-Gutiérrez, J. M.; López-Ortiz, F. Synthesis of 1H-1,2 Λ5-Azaphosphinin-6-Ones from N-Alkoxycarbonyl Phosphazenes and DMAD. *Tetrahedron Lett.* **1996**, *37* (16), 2841–2844. https://doi.org/10.1016/0040-4039(96)00401-7.
(90) Álvarez-Gutiérrez, J. M.; Peralta-Pérez, E.; Pérez-Álvarez, I.; López-Ortiz, F. Reactions of Lithiated P-Diphenyl(Alkyl)(N-Methoxycarbonyl)Phosphazenes with Michael Acceptors and Aldehydes. Synthesis of 1H-1,2-Azaphosphinin-6-Ones, β-Hydroxy(N-Methoxycarbonyl)Phosphazenes and 5,6-Dihydro-1,3,4-Oxazaphosphinin-2-Ones. *Tetrahedron* **2001**, *57* (15), 3075–3086. https://doi.org/10.1016/S0040-4020(01)00165-X.

SUMMARY IN ESTONIAN

Fosfaanide ja seotud ühendite aluselisus

Käesoleva doktoritöö eesmärk oli koondada erinevates allikates leiduvate fosfaanide aluselisuse andmed ühtseks ja terviklikuks ülevaateks ning käsitleda samas ka olemasolevates andmestikes esinevaid olulisi lünkasid. Lisaks taheti sünteesida uusi aluseid, millel on suhteliselt kõrge aluselisus ja sobivad UV-Vis spektraalomadused, eesmärgiga täiendada UV-Vis spektrofotomeetrilist aluselisuse skaalat atsetonitriilis.

Töös on esitatud pK_{aH} väärtused struktuuriliselt mitmekesisele fosfaanide ja seotud ühendite valikule, sealhulgas nii uusi mõõdetud või arvutatud väärtusi kui ka kirjandusest kogutud andmeid – kokku 80 pK_{aH} väärtust, neist 45 määratud arvutuslikult ja 22 eksperimentaalselt käesolevas töös, 13 eksperimentaalset väärtust võeti kirjandusest. Nagu töös näidatud, on fosfaanide aluselisust võimalik süsteemselt muuta asendajate modifitseerimise kaudu – pK_{aH} väärtused võivad ulatuda ligikaudu −30-st kuni üle 30-ni (atsetonitriilis). Elektron-aktseptoorsed asendajad langetavad fosfaanide pK_{aH} väärtust (vähendavad aluselisust), samas kui elektron-donoorsed rühmad suurendavad seda.

Töös pakutakse välja raamistik fosfaanide elektroonsete ja steeriliste omaduste hindamiseks. Tulemustest selgus, et pK_{aH} väärtused korreleeruvad hästi traditsiooniliste Tolmani elektroonsete parameetritega (TEP), mistõttu võiks pK_{aH} väärtusi kasutada praktilise alternatiivina fosfaanide elektroonsete omaduste hindamisel. Lisaks pakuti välja uued steerilised deskriptorid, mis võiksid asendada laialdaselt kasutatavat Tolmani koonusenurka, mille määramine on keerulisem. Esmases sõelumisetapis võib kasutada C–P–C nurki (θ_{CPC}) või protoneeritud fosfaanide koonusenurki (θ_H), sõltuvalt uuritavate ühendite komplektist. Nende väärtuste kasutamine võiks lihtsustada tulevikus ligandide sobivuse esmast hindamist, kõrvaldades vajaduse valmistada või arvutada metall-ligand komplekse kõikidele huvipakkuvatele fosfaanidele, tehes seda vaid enim potentsiaali näitavatele ligandidele.

Lisaks sünteesiti uued bensofenoonimino (bpi) rühma sisaldavad fosfaseenid, eksperimentaalsete pK_{aH} väärtustega vahemikus 17 kuni 26 atsetonitriilis. Kuigi paljud juba olemasolevad alused on kõrgema aluselisusega, on need bpi-fosfaseenid siiski piisavalt tugevad ning võivad potentsiaalselt pakkuda praktilisi eeliseid reaktiividena. Nende kasutamine võib aidata vältida mõningaid probleeme, nagu halb lahustuvus või UV-Vis aktiivsuse puudumine.

Hoolimata asjaolust, et bpi-fosfaseenid näitasid head stabiilsust, viis P(bpi)$_3$ protoneerimine unikaalse P-N heterotsükli moodustumiseni. Sama täheldati ka bpi-asendatud fosfooniumkatioonide deprotoneerimisel. See viitab nende ainete suurele steerilisele koormusele ja ebastabiilsusele.

Kokkuvõttes saavutati doktoritöö eesmärgid, koondades 63 fosfaani aluselisuse andmed ja steerilised omadused ühte tervikusse. Lisaks valmistati 15 uut bpi-ühendit, millest 9 uuele alusele mõõdeti ka eksperimentaalsed pK_{aH} väärtused. Aluselisuse väärtused määrati ka töös sünteesitud bpi-ühendite prekursoritele.

ACKNOWLEDGEMENTS

I would like to express my sincerest gratitude to my supervisors, Assoc. Prof. Agnes Kütt and Prof. Ivo Leito, for their invaluable guidance and support throughout my doctoral studies. Agnes, thank you for taking me under your wing at the beginning of my master's journey, for believing in me, and for offering support during challenging times. I am especially grateful for your kindness, for never making me feel inadequate when I asked naive questions, and for creating an environment where I always felt comfortable seeking your help. I also deeply appreciate the many conversations we shared beyond the realm of science. Ivo, thank you for your insightful comments, your remarkable work ethic, and your consistent willingness to discuss even the most detailed aspects of my work. Your open-door policy and patient explanations have been instrumental to my growth as a researcher.

I would also like to extend my heartfelt thanks to my past and present colleagues at the Chair of Analytical Chemistry. Sigrid, thank you not only for making the workdays more fun, but also for becoming one of my closest friends – I truly appreciate you (and your cooking). Märt and Elisabeth, thank you for being the best co-supervisors one could ask for, and for your wonderful company. Lauri, I am beyond grateful for your guidance in learning NMR. Sofja, thank you for patiently answering my many messages when yet another piece of software resisted cooperation (or maybe it was me).

A special shoutout to all doctoral students who have shared in the struggles and triumphs of my journey. Miriam and Heigo, thank you for being a safe space to vent and feel truly understood. Anu, thank you for reminding me that the challenges of academia are universal, even across the ocean.

Most of all, I would like to express my deepest gratitude to my family. To my parents, thank you for your unwavering support and for being my greatest cheerleaders – I would not be here without you (musi-kalli). I would also like to thank Piret, who has always been more like a sister than a sister-in-law to me in every sense. My choice of career speaks for itself – I have always looked up to you, admired your dedication and work ethic, and aspired to match your ability to work hard while never losing your sense of fun. I am incredibly thankful to you for everything. Thank you, Priit, for always making me feel loved and protected – as any awesome big brother would. Janne, Tiit, Nele – thank you to you as well for always being there for me.

And finally, the most special people in my life. Marten, thank you for standing by me during the hardest moments, for listening, and also for sharing in my laughter and joy when I am at my happiest (usually thanks to you). There is no one else I would rather walk through life with (sorry for not defending this thesis under my new name). Arkyn, you are the most precious and brightest light there could ever be, and my greatest inspiration. Thank you for honoring me with the greatest gift I will ever receive – making me a mom and filling my days with unimaginable happiness.

This work was supported by grant PRG1736 from the Estonian Research Council and by the Estonian Ministry of Education and Research (TK210). Quantum-chemical computations were carried out in the High Performance Computing Center of the University of Tartu. I acknowledge University of Tartu, Estonia for awarding me access to the LUMI supercomputer, owned by the EuroHPC Joint Undertaking, hosted by CSC (Finland) and the LUMI consortium through ETAIS, Estonia. This thesis has been partially supported by Graduate School of Functional materials and technologies receiving funding from the European Regional Development Fund in University of Tartu, Estonia.

PUBLICATIONS

CURRICULUM VITAE

Name: Marta-Lisette Vares (née Pikma)
Date of birth: March 11, 1997, Pärnu, Estonia
Citizenship: Estonia
Contact: University of Tartu, Institute of Chemistry, Ravila 14a, Tartu, 50411, Estonia
E-mail: marta.pikma@ut.ee

Education:

2021–…	University of Tartu, Institute of Chemistry, PhD (Chemistry)
2019–2021	University of Tartu, Institute of Chemistry, M.Sc. (Chemistry)
2016–2019	University of Tartu, Institute of Chemistry, B.Sc. (Physics, Chemistry, and Materials science)

Professional employment:

11.2021–…	Junior Research Fellow (0.4), University of Tartu, Institute of Chemistry

Scientific publications:

1. **Pikma, M.-L.**; Ilisson, M.; Zalite, R.; Lavogina, D.; Haljasorg, T.; Mäeorg, U. The Effect of Substituents on Carbon–Carbon Double Bond Isomerization in Heterocyclic Hydrazine Derivatives. *Chem. Heterocycl. Compd.* **2022**, *58* (4/5), 206–216.
2. **Pikma, M.-L.**; Lõkov, M.; Tshepelevitsh, S.; Saame, J.; Haljasorg, T.; Toom, L.; Selberg, S.; Leito, I.; Kütt, A. Tris(Benzophenoneimino)Phosphane and Related Compounds. *Eur. J. Org. Chem.* **2023**, *26* (28), e202300453.
3. **Pikma, M.-L.**; Tshepelevitsh, S.; Selberg, S.; Kaljurand, I.; Leito, I.; Kütt, A. pK_{aH} Values and θ_H Angles of Phosphanes to Predict Their Electronic and Steric Parameters. *Dalton Trans.* **2024**, *53* (34), 14226–14236.
4. Lõkov, M.; Kesküla, C.; Tshepelevitsh, S.; **Pikma, M.-L.**; Saame, J.; Trubitsõn, D.; Kanger, T.; Leito, I. The Acidity of Weak NH Acids: Expanding the pK_a Scale in Acetonitrile. *ACS Org. Inorg. Au* **2025**, *5* (2), 144–155.
5. **Pikma, M.-L.**; Trummal, A.; Leito, I.; Kütt, A. The Impact of Perfluoroalkyl Groups on Phosphane Basicity. *Molecules* **2025**, *30* (10), 2220.

Industrial property:

1. Kõiv, K.; Mölder, T.; Teesalu, T.; Tämm, K.; Tamm, T.; Põhako-Esko, K.; Lavõgina, D.; **Pikma, M.-L.**; Mäeorg, U.; Tahk, M.-J.; Laasfeld, T.; Rinken, A. Novel Peptide Conjugates. WO2024115720A1, June 6, 2024.

ELULOOKIRJELDUS

Nimi: Marta-Lisette Vares (sündinud Pikma)
Sünniaeg: 11. märts 1997, Pärnu, Eesti
Kodakondsus: Eesti
Kontakt: Tartu Ülikool, Keemia instituut, Ravila 14a, Tartu, 50411, Eesti
E-post: marta.pikma@ut.ee

Haridus:

2021–...	Tartu Ülikool, Keemia instituut, doktoriõpe (keemia)
2019–2021	Tartu Ülikool, Keemia instituut, magistriõpe (keemia)
2016–2019	Tartu Ülikool, Keemia instituut, bakalaureuseõpe (füüsika, keemia ja materjaliteadus)

Töökogemus:

11.2021–	Nooremteadur (0,4), Tartu Ülikool, Keemia instituut

Teaduspublikatsioonid:

1. **Pikma, M.-L.**; Ilisson, M.; Zalite, R.; Lavogina, D.; Haljasorg, T.; Mäeorg, U. The Effect of Substituents on Carbon–Carbon Double Bond Isomerization in Heterocyclic Hydrazine Derivatives. *Chem. Heterocycl. Compd.* **2022**, *58* (4/5), 206–216.
2. **Pikma, M.-L.**; Lõkov, M.; Tshepelevitsh, S.; Saame, J.; Haljasorg, T.; Toom, L.; Selberg, S.; Leito, I.; Kütt, A. Tris(Benzophenoneimino)Phosphane and Related Compounds. *Eur. J. Org. Chem.* **2023**, *26* (28), e202300453.
3. **Pikma, M.-L.**; Tshepelevitsh, S.; Selberg, S.; Kaljurand, I.; Leito, I.; Kütt, A. pK_{aH} Values and θ_H Angles of Phosphanes to Predict Their Electronic and Steric Parameters. *Dalton Trans.* **2024**, *53* (34), 14226–14236.
4. Lõkov, M.; Kesküla, C.; Tshepelevitsh, S.; **Pikma, M.-L.**; Saame, J.; Trubitsõn, D.; Kanger, T.; Leito, I. The Acidity of Weak NH Acids: Expanding the pK_a Scale in Acetonitrile. *ACS Org. Inorg. Au* **2025**, *5* (2), 144–155.
5. **Pikma, M.-L.**; Trummal, A.; Leito, I.; Kütt, A. The Impact of Perfluoroalkyl Groups on Phosphane Basicity. *Molecules* **2025**, *30* (10), 2220.

Tööstusomand:

1. Kõiv, K.; Mölder, T.; Teesalu, T.; Tämm, K.; Tamm, T.; Põhako-Esko, K.; Lavõgina, D.; **Pikma, M.-L.**; Mäeorg, U.; Tahk, M.-J.; Laasfeld, T.; Rinken, A. Novel Peptide Conjugates. WO2024115720A1, June 6, 2024.

DISSERTATIONES CHIMICAE UNIVERSITATIS TARTUENSIS

1. **Toomas Tamm.** Quantum-chemical simulation of solvent effects. Tartu, 1993, 110 p.
2. **Peeter Burk.** Theoretical study of gas-phase acid-base equilibria. Tartu, 1994, 96 p.
3. **Victor Lobanov.** Quantitative structure-property relationships in large descriptor spaces. Tartu, 1995, 135 p.
4. **Vahur Mäemets.** The ^{17}O and ^{1}H nuclear magnetic resonance study of H_2O in individual solvents and its charged clusters in aqueous solutions of electrolytes. Tartu, 1997, 140 p.
5. **Andrus Metsala.** Microcanonical rate constant in nonequilibrium distribution of vibrational energy and in restricted intramolecular vibrational energy redistribution on the basis of slater's theory of unimolecular reactions. Tartu, 1997, 150 p.
6. **Uko Maran.** Quantum-mechanical study of potential energy surfaces in different environments. Tartu, 1997, 137 p.
7. **Alar Jänes.** Adsorption of organic compounds on antimony, bismuth and cadmium electrodes. Tartu, 1998, 219 p.
8. **Kaido Tammeveski.** Oxygen electroreduction on thin platinum films and the electrochemical detection of superoxide anion. Tartu, 1998, 139 p.
9. **Ivo Leito.** Studies of Brønsted acid-base equilibria in water and non-aqueous media. Tartu, 1998, 101 p.
10. **Jaan Leis.** Conformational dynamics and equilibria in amides. Tartu, 1998, 131 p.
11. **Toonika Rinken.** The modelling of amperometric biosensors based on oxidoreductases. Tartu, 2000, 108 p.
12. **Dmitri Panov.** Partially solvated Grignard reagents. Tartu, 2000, 64 p.
13. **Kaja Orupõld.** Treatment and analysis of phenolic wastewater with microorganisms. Tartu, 2000, 123 p.
14. **Jüri Ivask.** Ion Chromatographic determination of major anions and cations in polar ice core. Tartu, 2000, 85 p.
15. **Lauri Vares.** Stereoselective Synthesis of Tetrahydrofuran and Tetrahydropyran Derivatives by Use of Asymmetric Horner-Wadsworth-Emmons and Ring Closure Reactions. Tartu, 2000, 184 p.
16. **Martin Lepiku.** Kinetic aspects of dopamine D_2 receptor interactions with specific ligands. Tartu, 2000, 81 p.
17. **Katrin Sak.** Some aspects of ligand specificity of P2Y receptors. Tartu, 2000, 106 p.
18. **Vello Pällin.** The role of solvation in the formation of iotsitch complexes. Tartu, 2001, 95 p.
19. **Katrin Kollist.** Interactions between polycyclic aromatic compounds and humic substances. Tartu, 2001, 93 p.

20. **Ivar Koppel.** Quantum chemical study of acidity of strong and superstrong Brønsted acids. Tartu, 2001, 104 p.
21. **Viljar Pihl.** The study of the substituent and solvent effects on the acidity of OH and CH acids. Tartu, 2001, 132 p.
22. **Natalia Palm.** Specification of the minimum, sufficient and significant set of descriptors for general description of solvent effects. Tartu, 2001, 134 p.
23. **Sulev Sild.** QSPR/QSAR approaches for complex molecular systems. Tartu, 2001, 134 p.
24. **Ruslan Petrukhin.** Industrial applications of the quantitative structure-property relationships. Tartu, 2001, 162 p.
25. **Boris V. Rogovoy.** Synthesis of (benzotriazolyl)carboximidamides and their application in relations with *N*- and *S*-nucleophyles. Tartu, 2002, 84 p.
26. **Koit Herodes.** Solvent effects on UV-vis absorption spectra of some solvatochromic substances in binary solvent mixtures: the preferential solvation model. Tartu, 2002, 102 p.
27. **Anti Perkson.** Synthesis and characterisation of nanostructured carbon. Tartu, 2002, 152 p.
28. **Ivari Kaljurand.** Self-consistent acidity scales of neutral and cationic Brønsted acids in acetonitrile and tetrahydrofuran. Tartu, 2003, 108 p.
29. **Karmen Lust.** Adsorption of anions on bismuth single crystal electrodes. Tartu, 2003, 128 p.
30. **Mare Piirsalu.** Substituent, temperature and solvent effects on the alkaline hydrolysis of substituted phenyl and alkyl esters of benzoic acid. Tartu, 2003, 156 p.
31. **Meeri Sassian.** Reactions of partially solvated Grignard reagents. Tartu, 2003, 78 p.
32. **Tarmo Tamm.** Quantum chemical modelling of polypyrrole. Tartu, 2003. 100 p.
33. **Erik Teinemaa.** The environmental fate of the particulate matter and organic pollutants from an oil shale power plant. Tartu, 2003. 102 p.
34. **Jaana Tammiku-Taul.** Quantum chemical study of the properties of Grignard reagents. Tartu, 2003. 120 p.
35. **Andre Lomaka.** Biomedical applications of predictive computational chemistry. Tartu, 2003. 132 p.
36. **Kostyantyn Kirichenko.** Benzotriazole – Mediated Carbon–Carbon Bond Formation. Tartu, 2003. 132 p.
37. **Gunnar Nurk.** Adsorption kinetics of some organic compounds on bismuth single crystal electrodes. Tartu, 2003, 170 p.
38. **Mati Arulepp.** Electrochemical characteristics of porous carbon materials and electrical double layer capacitors. Tartu, 2003, 196 p.
39. **Dan Cornel Fara.** QSPR modeling of complexation and distribution of organic compounds. Tartu, 2004, 126 p.
40. **Riina Mahlapuu.** Signalling of galanin and amyloid precursor protein through adenylate cyclase. Tartu, 2004, 124 p.

41. **Mihkel Kerikmäe.** Some luminescent materials for dosimetric applications and physical research. Tartu, 2004, 143 p.
42. **Jaanus Kruusma.** Determination of some important trace metal ions in human blood. Tartu, 2004, 115 p.
43. **Urmas Johanson.** Investigations of the electrochemical properties of polypyrrole modified electrodes. Tartu, 2004, 91 p.
44. **Kaido Sillar.** Computational study of the acid sites in zeolite ZSM-5. Tartu, 2004, 80 p.
45. **Aldo Oras.** Kinetic aspects of dATPαS interaction with $P2Y_1$ receptor. Tartu, 2004, 75 p.
46. **Erik Mölder.** Measurement of the oxygen mass transfer through the air-water interface. Tartu, 2005, 73 p.
47. **Thomas Thomberg.** The kinetics of electroreduction of peroxodisulfate anion on cadmium (0001) single crystal electrode. Tartu, 2005, 95 p.
48. **Olavi Loog.** Aspects of condensations of carbonyl compounds and their imine analogues. Tartu, 2005, 83 p.
49. **Siim Salmar.** Effect of ultrasound on ester hydrolysis in aqueous ethanol. Tartu, 2006, 73 p.
50. **Ain Uustare.** Modulation of signal transduction of heptahelical receptors by other receptors and G proteins. Tartu, 2006, 121 p.
51. **Sergei Yurchenko.** Determination of some carcinogenic contaminants in food. Tartu, 2006, 143 p.
52. **Kaido Tämm.** QSPR modeling of some properties of organic compounds. Tartu, 2006, 67 p.
53. **Olga Tšubrik.** New methods in the synthesis of multisubstituted hydrazines. Tartu. 2006, 183 p.
54. **Lilli Sooväli.** Spectrophotometric measurements and their uncertainty in chemical analysis and dissociation constant measurements. Tartu, 2006, 125 p.
55. **Eve Koort.** Uncertainty estimation of potentiometrically measured ph and pK_a values. Tartu, 2006, 139 p.
56. **Sergei Kopanchuk.** Regulation of ligand binding to melanocortin receptor subtypes. Tartu, 2006, 119 p.
57. **Silvar Kallip.** Surface structure of some bismuth and antimony single crystal electrodes. Tartu, 2006, 107 p.
58. **Kristjan Saal.** Surface silanization and its application in biomolecule coupling. Tartu, 2006, 77 p.
59. **Tanel Tätte.** High viscosity $Sn(OBu)_4$ oligomeric concentrates and their applications in technology. Tartu, 2006, 91 p.
60. **Dimitar Atanasov Dobchev**. Robust QSAR methods for the prediction of properties from molecular structure. Tartu, 2006, 118 p.
61. **Hannes Hagu**. Impact of ultrasound on hydrophobic interactions in solutions. Tartu, 2007, 81 p.
62. **Rutha Jäger.** Electroreduction of peroxodisulfate anion on bismuth electrodes. Tartu, 2007, 142 p.

63. **Kaido Viht.** Immobilizable bisubstrate-analogue inhibitors of basophilic protein kinases: development and application in biosensors. Tartu, 2007, 88 p.
64. **Eva-Ingrid Rõõm.** Acid-base equilibria in nonpolar media. Tartu, 2007, 156 p.
65. **Sven Tamp.** DFT study of the cesium cation containing complexes relevant to the cesium cation binding by the humic acids. Tartu, 2007, 102 p.
66. **Jaak Nerut.** Electroreduction of hexacyanoferrate(III) anion on Cadmium (0001) single crystal electrode. Tartu, 2007, 180 p.
67. **Lauri Jalukse.** Measurement uncertainty estimation in amperometric dissolved oxygen concentration measurement. Tartu, 2007, 112 p.
68. **Aime Lust.** Charge state of dopants and ordered clusters formation in CaF_2:Mn and CaF_2:Eu luminophors. Tartu, 2007, 100 p.
69. **Iiris Kahn**. Quantitative Structure-Activity Relationships of environmentally relevant properties. Tartu, 2007, 98 p.
70. **Mari Reinik.** Nitrates, nitrites, N-nitrosamines and polycyclic aromatic hydrocarbons in food: analytical methods, occurrence and dietary intake. Tartu, 2007, 172 p.
71. **Heili Kasuk.** Thermodynamic parameters and adsorption kinetics of organic compounds forming the compact adsorption layer at Bi single crystal electrodes. Tartu, 2007, 212 p.
72. **Erki Enkvist.** Synthesis of adenosine-peptide conjugates for biological applications. Tartu, 2007, 114 p.
73. **Svetoslav Hristov Slavov**. Biomedical applications of the QSAR approach. Tartu, 2007, 146 p.
74. **Eneli Härk.** Electroreduction of complex cations on electrochemically polished Bi(*hkl*) single crystal electrodes. Tartu, 2008, 158 p.
75. **Priit Möller.** Electrochemical characteristics of some cathodes for medium temperature solid oxide fuel cells, synthesized by solid state reaction technique. Tartu, 2008, 90 p.
76. **Signe Viggor.** Impact of biochemical parameters of genetically different pseudomonads at the degradation of phenolic compounds. Tartu, 2008, 122 p.
77. **Ave Sarapuu.** Electrochemical reduction of oxygen on quinone-modified carbon electrodes and on thin films of platinum and gold. Tartu, 2008, 134 p.
78. **Agnes Kütt.** Studies of acid-base equilibria in non-aqueous media. Tartu, 2008, 198 p.
79. **Rouvim Kadis.** Evaluation of measurement uncertainty in analytical chemistry: related concepts and some points of misinterpretation. Tartu, 2008, 118 p.
80. **Valter Reedo.** Elaboration of IVB group metal oxide structures and their possible applications. Tartu, 2008, 98 p.
81. **Aleksei Kuznetsov.** Allosteric effects in reactions catalyzed by the cAMP-dependent protein kinase catalytic subunit. Tartu, 2009, 133 p.

82. **Aleksei Bredihhin.** Use of mono- and polyanions in the synthesis of multisubstituted hydrazine derivatives. Tartu, 2009, 105 p.
83. **Anu Ploom.** Quantitative structure-reactivity analysis in organosilicon chemistry. Tartu, 2009, 99 p.
84. **Argo Vonk.** Determination of adenosine A_{2A}- and dopamine D_1 receptor-specific modulation of adenylate cyclase activity in rat striatum. Tartu, 2009, 129 p.
85. **Indrek Kivi.** Synthesis and electrochemical characterization of porous cathode materials for intermediate temperature solid oxide fuel cells. Tartu, 2009, 177 p.
86. **Jaanus Eskusson.** Synthesis and characterisation of diamond-like carbon thin films prepared by pulsed laser deposition method. Tartu, 2009, 117 p.
87. **Marko Lätt.** Carbide derived microporous carbon and electrical double layer capacitors. Tartu, 2009, 107 p.
88. **Vladimir Stepanov.** Slow conformational changes in dopamine transporter interaction with its ligands. Tartu, 2009, 103 p.
89. **Aleksander Trummal.** Computational Study of Structural and Solvent Effects on Acidities of Some Brønsted Acids. Tartu, 2009, 103 p.
90. **Eerold Vellemäe.** Applications of mischmetal in organic synthesis. Tartu, 2009, 93 p.
91. **Sven Parkel.** Ligand binding to 5-HT_{1A} receptors and its regulation by Mg^{2+} and Mn^{2+}. Tartu, 2010, 99 p.
92. **Signe Vahur.** Expanding the possibilities of ATR-FT-IR spectroscopy in determination of inorganic pigments. Tartu, 2010, 184 p.
93. **Tavo Romann**. Preparation and surface modification of bismuth thin film, porous, and microelectrodes. Tartu, 2010, 155 p.
94. **Nadežda Aleksejeva.** Electrocatalytic reduction of oxygen on carbon nanotube-based nanocomposite materials. Tartu, 2010, 147 p.
95. **Marko Kullapere.** Electrochemical properties of glassy carbon, nickel and gold electrodes modified with aryl groups. Tartu, 2010, 233 p.
96. **Liis Siinor.** Adsorption kinetics of ions at Bi single crystal planes from aqueous electrolyte solutions and room-temperature ionic liquids. Tartu, 2010, 101 p.
97. **Angela Vaasa.** Development of fluorescence-based kinetic and binding assays for characterization of protein kinases and their inhibitors. Tartu 2010, 101 p.
98. **Indrek Tulp.** Multivariate analysis of chemical and biological properties. Tartu 2010, 105 p.
99. **Aare Selberg.** Evaluation of environmental quality in Northern Estonia by the analysis of leachate. Tartu 2010, 117 p.
100. **Darja Lavõgina.** Development of protein kinase inhibitors based on adenosine analogue-oligoarginine conjugates. Tartu 2010, 248 p.
101. **Laura Herm.** Biochemistry of dopamine D_2 receptors and its association with motivated behaviour. Tartu 2010, 156 p.

102. **Terje Raudsepp.** Influence of dopant anions on the electrochemical properties of polypyrrole films. Tartu 2010, 112 p.
103. **Margus Marandi.** Electroformation of Polypyrrole Films: *In-situ* AFM and STM Study. Tartu 2011, 116 p.
104. **Kairi Kivirand.** Diamine oxidase-based biosensors: construction and working principles. Tartu, 2011, 140 p.
105. **Anneli Kruve.** Matrix effects in liquid-chromatography electrospray mass-spectrometry. Tartu, 2011, 156 p.
106. **Gary Urb.** Assessment of environmental impact of oil shale fly ash from PF and CFB combustion. Tartu, 2011, 108 p.
107. **Nikita Oskolkov.** A novel strategy for peptide-mediated cellular delivery and induction of endosomal escape. Tartu, 2011, 106 p.
108. **Dana Martin.** The QSPR/QSAR approach for the prediction of properties of fullerene derivatives. Tartu, 2011, 98 p.
109. **Säde Viirlaid.** Novel glutathione analogues and their antioxidant activity. Tartu, 2011, 106 p.
110. **Ülis Sõukand.** Simultaneous adsorption of Cd^{2+}, Ni^{2+}, and Pb^{2+} on peat. Tartu, 2011, 124 p.
111. **Lauri Lipping.** The acidity of strong and superstrong Brønsted acids, an outreach for the "limits of growth": a quantum chemical study. Tartu, 2011, 124 p.
112. **Heisi Kurig.** Electrical double-layer capacitors based on ionic liquids as electrolytes. Tartu, 2011, 146 p.
113. **Marje Kasari.** Bisubstrate luminescent probes, optical sensors and affinity adsorbents for measurement of active protein kinases in biological samples. Tartu, 2012, 126 p.
114. **Kalev Takkis.** Virtual screening of chemical databases for bioactive molecules. Tartu, 2012, 122 p.
115. **Ksenija Kisseljova**. Synthesis of aza-β^3-amino acid containing peptides and kinetic study of their phosphorylation by protein kinase A. Tartu, 2012, 104 p.
116. **Riin Rebane.** Advanced method development strategy for derivatization LC/ESI/MS. Tartu, 2012, 184 p.
117. **Vladislav Ivaništšev.** Double layer structure and adsorption kinetics of ions at metal electrodes in room temperature ionic liquids. Tartu, 2012, 128 p.
118. **Irja Helm.** High accuracy gravimetric Winkler method for determination of dissolved oxygen. Tartu, 2012, 139 p.
119. **Karin Kipper.** Fluoroalcohols as Components of LC-ESI-MS Eluents: Usage and Applications. Tartu, 2012, 164 p.
120. **Arno Ratas.** Energy storage and transfer in dosimetric luminescent materials. Tartu, 2012, 163 p.
121. **Reet Reinart-Okugbeni**. Assay systems for characterisation of subtype-selective binding and functional activity of ligands on dopamine receptors. Tartu, 2012, 159 p.

122. **Lauri Sikk.** Computational study of the Sonogashira cross-coupling reaction. Tartu, 2012, 81 p.
123. **Karita Raudkivi.** Neurochemical studies on inter-individual differences in affect-related behaviour of the laboratory rat. Tartu, 2012, 161 p.
124. **Indrek Saar.** Design of GalR2 subtype specific ligands: their role in depression-like behavior and feeding regulation. Tartu, 2013, 126 p.
125. **Ann Laheäär.** Electrochemical characterization of alkali metal salt based non-aqueous electrolytes for supercapacitors. Tartu, 2013, 127 p.
126. **Kerli Tõnurist.** Influence of electrospun separator materials properties on electrochemical performance of electrical double-layer capacitors. Tartu, 2013, 147 p.
127. **Kaija Põhako-Esko.** Novel organic and inorganic ionogels: preparation and characterization. Tartu, 2013, 124 p.
128. **Ivar Kruusenberg.** Electroreduction of oxygen on carbon nanomaterial-based catalysts. Tartu, 2013, 191 p.
129. **Sander Piiskop.** Kinetic effects of ultrasound in aqueous acetonitrile solutions. Tartu, 2013, 95 p.
130. **Ilona Faustova**. Regulatory role of L-type pyruvate kinase N-terminal domain. Tartu, 2013, 109 p.
131. **Kadi Tamm.** Synthesis and characterization of the micro-mesoporous anode materials and testing of the medium temperature solid oxide fuel cell single cells. Tartu, 2013, 138 p.
132. **Iva Bozhidarova Stoyanova-Slavova.** Validation of QSAR/QSPR for regulatory purposes. Tartu, 2013, 109 p.
133. **Vitali Grozovski**. Adsorption of organic molecules at single crystal electrodes studied by *in situ* STM method. Tartu, 2014, 146 p.
134. **Santa Veikšina**. Development of assay systems for characterisation of ligand binding properties to melanocortin 4 receptors. Tartu, 2014, 151 p.
135. **Jüri Liiv.** PVDF (polyvinylidene difluoride) as material for active element of twisting-ball displays. Tartu, 2014, 111 p.
136. **Kersti Vaarmets.** Electrochemical and physical characterization of pristine and activated molybdenum carbide-derived carbon electrodes for the oxygen electroreduction reaction. Tartu, 2014, 131 p.
137. **Lauri Tõntson**. Regulation of G-protein subtypes by receptors, guanine nucleotides and Mn^{2+}. Tartu, 2014, 105 p.
138. **Aiko Adamson.** Properties of amine-boranes and phosphorus analogues in the gas phase. Tartu, 2014, 78 p.
139. **Elo Kibena**. Electrochemical grafting of glassy carbon, gold, highly oriented pyrolytic graphite and chemical vapour deposition-grown graphene electrodes by diazonium reduction method. Tartu, 2014, 184 p.
140. **Teemu Näykki.** Novel Tools for Water Quality Monitoring – From Field to Laboratory. Tartu, 2014, 202 p.
141. **Karl Kaupmees.** Acidity and basicity in non-aqueous media: importance of solvent properties and purity. Tartu, 2014, 128 p.

142. **Oleg Lebedev**. Hydrazine polyanions: different strategies in the synthesis of heterocycles. Tartu, 2015, 118 p.
143. **Geven Piir.** Environmental risk assessment of chemicals using QSAR methods. Tartu, 2015, 123 p.
144. **Olga Mazina.** Development and application of the biosensor assay for measurements of cyclic adenosine monophosphate in studies of G protein-coupled receptor signalinga. Tartu, 2015, 116 p.
145. **Sandip Ashokrao Kadam.** Anion receptors: synthesis and accurate binding measurements. Tartu, 2015, 116 p.
146. **Indrek Tallo.** Synthesis and characterization of new micro-mesoporous carbide derived carbon materials for high energy and power density electrical double layer capacitors. Tartu, 2015, 148 p.
147. **Heiki Erikson.** Electrochemical reduction of oxygen on nanostructured palladium and gold catalysts. Tartu, 2015, 204 p.
148. **Erik Anderson.** *In situ* Scanning Tunnelling Microscopy studies of the interfacial structure between Bi(111) electrode and a room temperature ionic liquid. Tartu, 2015, 118 p.
149. **Girinath G. Pillai.** Computational Modelling of Diverse Chemical, Biochemical and Biomedical Properties. Tartu, 2015, 140 p.
150. **Piret Pikma.** Interfacial structure and adsorption of organic compounds at Cd(0001) and Sb(111) electrodes from ionic liquid and aqueous electrolytes: an *in situ* STM study. Tartu, 2015, 126 p.
151. **Ganesh babu Manoharan.** Combining chemical and genetic approaches for photoluminescence assays of protein kinases. Tartu, 2016, 126 p.
152. **Carolin Siimenson**. Electrochemical characterization of halide ion adsorption from liquid mixtures at Bi(111) and pyrolytic graphite electrode surface. Tartu, 2016, 110 p.
153. **Asko Laaniste.** Comparison and optimisation of novel mass spectrometry ionisation sources. Tartu, 2016, 156 p.
154. **Hanno Evard.** Estimating limit of detection for mass spectrometric analysis methods. Tartu, 2016, 224 p.
155. **Kadri Ligi.** Characterization and application of protein kinase-responsive organic probes with triplet-singlet energy transfer. Tartu, 2016, 122 p.
156. **Margarita Kagan.** Biosensing penicillins' residues in milk flows. Tartu, 2016, 130 p.
157. **Marie Kriisa.** Development of protein kinase-responsive photoluminescent probes and cellular regulators of protein phosphorylation. Tartu, 2016, 106 p.
158. **Mihkel Vestli.** Ultrasonic spray pyrolysis deposited electrolyte layers for intermediate temperature solid oxide fuel cells. Tartu, 2016, 156 p.
159. **Silver Sepp**. Influence of porosity of the carbide-derived carbon on the properties of the composite electrocatalysts and characteristics of polymer electrolyte fuel cells. Tartu, 2016, 137 p.
160. **Kristjan Haav**. Quantitative relative equilibrium constant measurements in supramolecular chemistry. Tartu, 2017, 158 p.

161. **Anu Teearu**. Development of MALDI-FT-ICR-MS methodology for the analysis of resinous materials. Tartu, 2017, 205 p.
162. **Taavi Ivan**. Bifunctional inhibitors and photoluminescent probes for studies on protein complexes. Tartu, 2017, 140 p.
163. **Maarja-Liisa Oldekop**. Characterization of amino acid derivatization reagents for LC-MS analysis. Tartu, 2017, 147 p.
164. **Kristel Jukk**. Electrochemical reduction of oxygen on platinum- and palladium-based nanocatalysts. Tartu, 2017, 250 p.
165. **Siim Kukk**. Kinetic aspects of interaction between dopamine transporter and *N*-substituted nortropane derivatives. Tartu, 2017, 107 p.
166. **Birgit Viira**. Design and modelling in early drug development in targeting HIV-1 reverse transcriptase and Malaria. Tartu, 2017, 172 p.
167. **Rait Kivi**. Allostery in cAMP dependent protein kinase catalytic subunit. Tartu, 2017, 115 p.
168. **Agnes Heering**. Experimental realization and applications of the unified acidity scale. Tartu, 2017, 123 p.
169. **Delia Juronen**. Biosensing system for the rapid multiplex detection of mastitis-causing pathogens in milk. Tartu, 2018, 85 p.
170. **Hedi Rahnel.** ARC-inhibitors: from reliable biochemical assays to regulators of physiology of cells. Tartu, 2018, 176 p.
171. **Anton Ruzanov.** Computational investigation of the electrical double layer at metal–aqueous solution and metal–ionic liquid interfaces. Tartu, 2018, 129 p.
172. **Katrin Kestav.** Crystal Structure-Guided Development of Bisubstrate-Analogue Inhibitors of Mitotic Protein Kinase Haspin. Tartu, 2018, 166 p.
173. **Mihkel Ilisson.** Synthesis of novel heterocyclic hydrazine derivatives and their conjugates. Tartu, 2018, 101 p.
174. **Anni Allikalt.** Development of assay systems for studying ligand binding to dopamine receptors. Tartu, 2018, 160 p.
175. **Ove Oll.** Electrical double layer structure and energy storage characteristics of ionic liquid based capacitors. Tartu, 2018, 187 p.
176. **Rasmus Palm.** Carbon materials for energy storage applications. Tartu, 2018, 114 p.
177. **Jörgen Metsik.** Preparation and stability of poly(3,4-ethylenedioxythiophene) thin films for transparent electrode applications. Tartu, 2018, 111 p.
178. **Sofja Tšepelevitš.** Experimental studies and modeling of solute-solvent interactions. Tartu, 2018, 109 p.
179. **Märt Lõkov.** Basicity of some nitrogen, phosphorus and carbon bases in acetonitrile. Tartu, 2018, 104 p.
180. **Anton Mastitski**. Preparation of α-aza-amino acid precursors and related compounds by novel methods of reductive one-pot alkylation and direct alkylation. Tartu, 2018, 155 p.
181. **Jürgen Vahter**. Development of bisubstrate inhibitors for protein kinase CK2. Tartu, 2019, 186 p.

182. **Piia Liigand.** Expanding and improving methodology and applications of ionization efficiency measurements. Tartu, 2019, 189 p.
183. **Sigrid Selberg.** Synthesis and properties of lipophilic phosphazene-based indicator molecules. Tartu, 2019, 74 p.
184. **Jaanus Liigand.** Standard substance free quantification for LC/ESI/MS analysis based on the predicted ionization efficiencies. Tartu, 2019, 254 p.
185. **Marek Mooste.** Surface and electrochemical characterisation of aryl film and nanocomposite material modified carbon and metal-based electrodes. Tartu, 2019, 304 p.
186. **Mare Oja.** Experimental investigation and modelling of pH profiles for effective membrane permeability of drug substances. Tartu, 2019, 306 p.
187. **Sajid Hussain.** Electrochemical reduction of oxygen on supported Pt catalysts. Tartu, 2019, 220 p.
188. **Ronald Väli.** Glucose-derived hard carbon electrode materials for sodium-ion batteries. Tartu, 2019, 180 p.
189. **Ester Tee.** Analysis and development of selective synthesis methods of hierarchical micro- and mesoporous carbons. Tartu, 2019, 210 p.
190. **Martin Maide.** Influence of the microstructure and chemical composition of the fuel electrode on the electrochemical performance of reversible solid oxide fuel cell. Tartu, 2020, 144 p.
191. **Edith Viirlaid.** Biosensing Pesticides in Water Samples. Tartu, 2020, 102 p.
192. **Maike Käärik.** Nanoporous carbon: the controlled nanostructure, and structure-property relationships. Tartu, 2020, 162 p.
193. **Artur Gornischeff.** Study of ionization efficiencies for derivatized compounds in LC/ESI/MS and their application for targeted analysis. Tartu, 2020, 124 p.
194. **Reet Link.** Ligand binding, allosteric modulation and constitutive activity of melanocortin-4 receptors. Tartu, 2020, 108 p.
195. **Pilleriin Peets.** Development of instrumental methods for the analysis of textile fibres and dyes. Tartu, 2020, 150 p.
196. **Larisa Ivanova.** Design of active compounds against neurodegenerative diseases. Tartu, 2020, 152 p.
197. **Meelis Härmas.** Impact of activated carbon microstructure and porosity on electrochemical performance of electrical double-layer capacitors. Tartu, 2020, 122 p.
198. **Ruta Hecht.** Novel Eluent Additives for LC-MS Based Bioanalytical Methods. Tartu, 2020, 202 p.
199. **Max Hecht.** Advances in the Development of a Point-of-Care Mass Spectrometer Test. Tartu, 2020, 168 p.
200. **Ida Rahu.** Bromine formation in inorganic bromide/nitrate mixtures and its application for oxidative aromatic bromination. Tartu, 2020, 116 p.
201. **Sander Ratso**. Electrocatalysis of oxygen reduction on non-precious metal catalysts. Tartu, 2020, 371 p.
202. **Astrid Darnell.** Computational design of anion receptors and evaluation of host-guest binding. Tartu, 2021, 150 p.

203. **Ove Korjus.** The development of ceramic fuel electrode for solid oxide cells. Tartu, 2021, 150 p.
204. **Merit Oss.** Ionization efficiency in electrospray ionization source and its relations to compounds' physico-chemical properties. Tartu, 2021, 124 p.
205. **Madis Lüsi**. Electroreduction of oxygen on nanostructured palladium catalysts. Tartu, 2021, 180 p.
206. **Eliise Tammekivi.** Derivatization and quantitative gas-chromatographic analysis of oils. Tartu, 2021, 122 p.
207. **Simona Selberg.** Development of Small-Molecule Regulators of Epi-transcriptomic Processes. Tartu, 2021, 122 p.
208. **Olivier Etebe Nonga.** Inhibitors and photoluminescent probes for in vitro studies on protein kinases PKA and PIM. Tartu, 2021, 189 p.
209. **Riinu Härmas.** The structure and H2 diffusion in porous carbide-derived carbon particles. Tartu, 2022, 123 p.
210. **Maarja Paalo.** Synthesis and characterization of novel carbon electrodes for high power density electrochemical capacitors. Tartu, 2022, 144 p.
211. **Jinfeng Zhao.** Electrochemical characteristics of Bi(hkl) and micro-meso-porous carbon electrodes in ionic liquid based electrolytes. Tartu, 2022, 134 p.
212. **Alar Heinsaar.** Investigation of oxygen electrode materials for high-temperature solid oxide cells in natural conditions. Tartu, 2022, 120 p.
213. **Jaana Lilloja.** Transition metal and nitrogen doped nanocarbon cathode catalysts for anion exchange membrane fuel cells. Tartu, 2022, 202 p.
214. **Maris-Johanna Tahk.** Novel fluorescence-based methods for illuminating transmembrane signal transduction by G-protein coupled receptors. Tartu, 2022, 200 p.
215. **Eerik Jõgi.** Development and Applications of E. coli Immunosensor. Tartu, 2022, 103 p.
216. **Alo Rüütel.** Design principles of synthetic molecular receptors for anion-selective electrodes. Tartu, 2022, 109 p.
217. **Tanel Sõrmus.** Development of stimuli-responsive and covalent bisubstrate inhibitors of protein kinases. Tartu, 2022, 148 p.
218. **Oleg Artemchuk.** Autotrophic nitrogen removal processes for nutrient removal from sidestream and mainstream wastewater. Tartu, 2022, 115 p.
219. **Andre Leesment.** Quantitative studies of Brønsted acidity in biphasic systems and gas-phase. Tartu, 2023, 83 p.
220. **Meeli Arujõe-Sado.** Structural effects in aza-peptide bond formation reaction. Tartu, 2023, 83 p.
221. **Jonas Mart Linge.** Electrochemical reduction of oxygen on silver-based catalysts. Tartu, 2023, 269 p.
222. **Tõnis Laasfeld.** Integrating Image Analysis and Quantitative Modeling for a Holistic View of GPCR Ligand Binding Dynamics. Tartu, 2023, 226 p.
223. **Ernesto de Jesus Zapata Flores.** Derivatization Reagents used in negative mode electrospray LC-MS. Tartu, 2023, 107 p.

224. **Patrick Teppor.** Obtaining platinum-free oxygen reduction catalysts through biomass valorization: a case study of peat. Tartu, 2023, 161 p.
225. **Peeter Valk.** Methanol Oxidation on Platinum-Rare-Earth Metal Oxide Activated Catalysts. Tartu, 2023, 162 p.
226. **Shidong Chen.** Unravelling prehistoric plant exploitation in eastern Baltic: organic residue analysis of plant-based materials by multi-method approach. Tartu, 2023, 245 p.
227. **Yogesh Kumar.** M-N_4 macrocycle-based catalysts for electrocatalysis of oxygen reduction and oxygen evolution. Tartu, 2023, 224 p.
228. **Kerli Martin.** Recognition of carboxylates by synthetic receptors – from structure-affinity studies to solid-contact anion-selective electrode prototyping. Tartu, 2024, 130 p.
229. **Huy Quí Vinh Nguyen.** Development of Carbon Supported Pt–CeO_2 Catalysts for Proton Exchange Membrane Fuel Cells. Tartu, 2024, 198 p.
230. **Heigo Ers**. Adsorption and Structuring Processes at Single Crystal Electrode – Ionic Liquid Interface – Insights from Simulations and *in situ* Studies. Tartu, 2024, 137 p.
231. **Ritums Cepitis.** Modelling Structural and Geometrical Effects in Carbon Dioxide and Oxygen Electrocatalysis. Tartu, 2024, 99 p.
232. **Kaarel Kisand.** Resorcinol-derived carbon-based catalysts for polymer electrolyte fuel cell cathodes. Tartu, 2024, 205 p.
233. **Akmal Kosimov**. Template-assisted Mechanosynthesis (TAMS) for the production of bifunctional transition metal-based catalysts. Tartu, 2024, 123 p.
234. **Larissa Silva Macieli.** Derivatization-targeted LC-MS analysis of compounds containing amino group. Tartu, 2024, 157 p.
235. **Silvester Jürjo.** Separation of rare earth elements from Estonian phosphorite ore using liquid extraction followed by electrochemical reduction. Tartu, 2024, 99 p.
236. **Jan-Michael C. Cayme.** Organic-inorganic interactions in experimental and archaeological ceramics. Tartu, 2025, 156 p.
237. **Miriam Koppel.** The diffusion of H2 adsorbed in carbide-derived carbons: a quasi-elastic neutron scattering study. Tartu, 2025, 138 p.
238. **Kenneth Tuul.** Evaluating lithium-ion pouch cells and hydrogen storage materials under extreme conditions using advanced techniques. Tartu, 2025, 188 p.